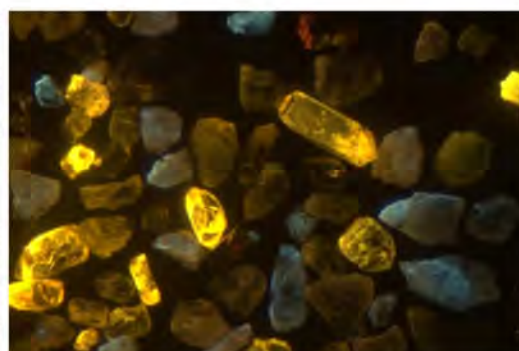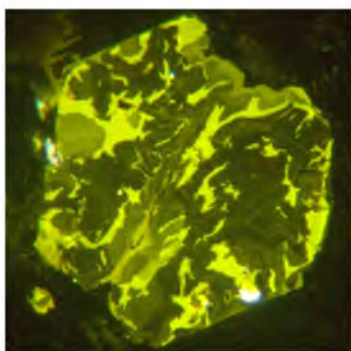# Porphyry Indicator Minerals (PIMS): A New Exploration Tool for Concealed Deposits in south-central British Columbia

Farhad Bouzari, Craig JR Hart, Shaun Barker and Thomas Bissig

Mineral Deposit Research Unit

Department of Earth and Ocean Sciences
The University of British Columbia
6339 Stores Road
Vancouver, BC V6T 1Z4
CANADA
mdru@eos.ubc.ca

MDRU

Mineral Deposit Research Unit
UBC

Table of Contents

EXECUTIVE SUMMARY

The common occurrence of resistate minerals, such as apatite, rutile, titanite and titanomagnetite, as alteration products in BC porphyry copper deposits suggest that these minerals could be utilized as porphyry indicator minerals (PIMS) and potentially provide a new exploration tool for BC explorers. The research project evaluated several resistate minerals but focused mainly on apatite and Fe-oxide phases from the Highland Valley, Mt. Polley, Mount Milligan, Huckleberry, Lorraine and Endako porphyry deposits. This research project has successfully recognized, characterized and documented the occurrence, types, relative abundances and compositions of selected resistate minerals in several BC porphyry deposits, such that the "proof of concept" of PIMS has been established. In short, we can now recognize features of resistate minerals that indicate their association with mineralized porphyry systems. This tool will be particularly beneficial in improving exploration targeting in terrains covered by glacial till.

Apatite occurs as grains 50 to 200 μm long in both fresh and altered host-rocks. Under visible light, the binocular microscope and the SEM, there are no notable differences between apatite in fresh and altered rocks, however significant differences in their characteristics are easily observable under cathodoluminescence. Apatite in fresh rocks associated with porphyry deposits displays yellow, yellow-brown and brown luminescence. Apatite associated with K-silicate altered host-rock in all studies deposits displays characteristic green luminescence. The green-luminescent apatite replaces yellow or brown-luminescent apatite and less commonly overgrows it. Apatite associated with muscovite alteration displays characteristic grey luminescence.

The chemistry of the apatites reflect their alteration and luminescence. The yellow luminescent apatite reflects its high concentrations of Mn, while the brown-luminescent apatite has low Mn, but higher concentrations of Cl, S and probably REE. The green luminescence is caused by lower Mn/Fe ratio. Other trace elements such as Cl, S, and Na were also depleted during K-silicate alteration. Grey luminescent apatite with muscovite alteration is the result of significant Mn and trace element loss during low pH phyllic alteration. Such apatites are not expected widely in alkalic deposits because such fluids were not developed in alkalic porphyry deposits.

Magnetite occurs as a common accessory mineral in the host-rocks of BC porphyry deposits and displays uniform pink color when examined under reflected light (e.g. titanomagnetite). Magnetite in fresh rocks hosting porphyry deposits has a characteristic rim of hematite or titanite which is interpreted as evidence of an increasing oxidation state of the late crystallizing melts which led to the generation of the porphyry deposit. Magnetite grains associated with altered host-rocks in all studied porphyry deposits display remnant of pink magnetite replaced by hematite indicating that the oxidation state of the porphyry systems progressively increased to stabilize hematite during the transition from K-silicate to sericite or chlorite alteration. The Ti from titanomagnetite commonly forms rutile lamella or grains within or near magnetite-hematite bodies. More advanced stages of magnetite alteration forms spongy hematite, with rutile, cemented by hydrothermal quartz thus forming more resistate aggregates.

These textural observations and chemical characteristics indicate that the footprints of porphyry-related alteration on apatite and Fe-oxide phases can provide a unique and reliable tool to search for porphyry deposits. The correlation between apatite luminescence and magnetite replacement textures with the degree and intensity of porphyry alteration offers a fast and effective method to utilize these minerals as indicators for porphyry mineralization in the weathered environment.

INTRODUCTION

Resistate minerals are those robust accessory minerals that persist through weathering in the surficial environment. Their presence in surficial materials have been successfully used to indicate the locations of kimberlite pipes in the exploration for diamonds (e.g., Griffin and Ryan, 1995; Averill, 2001; McClenaghan and Kjarsgaard, 2007). Although easy to collect in heavy mineral concentrates, resistate minerals have only rarely been used as exploration tools for other deposit types, including porphyry copper deposits (e.g., Force et al., 1984). Commonly occurring resistate minerals in alteration products in British Columbia porphyry copper deposits have the potential to become porphyry indicator minerals (PIMS) and improve mineral exploration effectiveness for porphyry deposits, especially in regions of prospective geology covered by glacial till.

The Quesnel and Stikine terranes in south-central BC comprise Late Triassic–Early Jurassic magmatic arcs that host several porphyry Cu±Mo and Cu-Au deposits. However, exploration success in large parts of these terranes has been limited due to extensive coverage by veneers of till and related glacial sediments (Ward et al., 2009), especially between the Mount Milligan and Mount Polley porphyry deposits (Figure 1). Geophysical and geochemical surveys in this region (e.g., Jackaman et al., 2009; Farr et al,, 2008; Kowalczyk, 2009) suggest that a broad correlation exists between the characteristics of stream and lake sediment geochemistry in the covered areas and the underlying bedrock geology (Barnett and Williams, 2009), thus indicating that the glacial sediments are not far travelled and homogenized, and are broadly reprehensive of the underlying bedrock. Therefore, the rock and mineral detritus in the sediments is also likely not far travelled and the presence of porphyry indicator minerals in these sediments could provide indications of proximal porphyry copper mineralization. Given that the volume of altered rocks in porphyry deposits is measured in square kilometres, minerals associated to alteration are also likely to be present in surficial sediments over a large territory. However, the nature, character and abundances of these individual potential porphyry indicator minerals are not known, and the overall indicator mineral signature of an eroding porphyry deposits is also not known.

The purpose of this research project was to evaluate the occurrence, types, relative abundances and composition of PIMS in selected porphyry deposits in order to provide a "proof of concept" result for the potential utility of PIMS
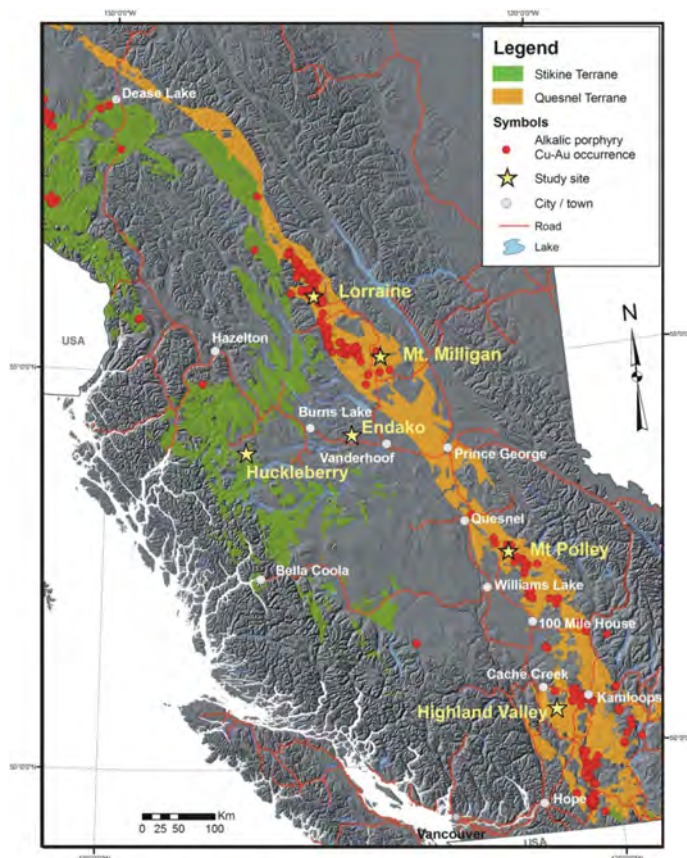
Figure 1: Outcrop distributions of Late Triassic and Early Jurassic Quesnel and Stikine terranes of south-central British Columbia (modified from Tosdal et al., 2008), and the locations of porphyry deposits selected for this study. Note the gap in the occurrence of deposits in the area between the Mount Polley and Mount Milligan deposits.

in porphyry exploration in BC. The main questions for consideration were: What resistate minerals could be key indicators of porphyry copper deposits? What are the characteristic features of PIMS, with emphasis on their physical appearance? Do these PIMS have a characteristic geochemical signature? Can we develop methods to optimize their evaluation in exploration? There are additional questions about PIMS sampling and application and distribution in surficial materials, but this is beyond the scope of this project.

The key objectives of the project were therefore to:

- determine the occurrence and types of resistate minerals related to various styles of mineralization and alteration in central BC porphyry copper-gold deposits;
- determine the diagnostic physical parameters and chemical compositions of these resistate minerals;
- identify the important resistate minerals as PIMS and

to establish their key physical properties so that they can be easily recognized and distinguished; and

- establish criteria for use of PIMS as an exploration tool in central BC.

Our results indicate that there are specific minerals that have characteristics that would easily identify them as PIMS. We obtained and herein present results on the physical and geochemical characteristics of apatite and magnetite-hematite that are associated with mineralized and barren host-rocks from several BC porphyry copper deposits. These results suggest that apatite and Fe-oxide minerals that form within, or are modified by porphyry copper mineralization, have distinct physical and chemical properties that can easily distinguish them from those associated with barren host rocks.

GEOLOGICAL SETTING

Cordilleran porphyry deposits have a diverse range of architecture, mineralization and alteration styles. These deposits formed during two separate time periods; Late Triassic to Middle Jurassic and Late Cretaceous to Eocene. The Early Mesozoic deposits include associations with both calc-alkalic and alkalic igneous rocks. Calc-alkalic varieties include the Island Copper Cu-Mo-Au, Highland Valley and Kemess Cu-Mo (McMillan et al., 1995). The alkalic Cu-Au deposits include Galore Creek, Mt. Milligan, Mt. Polley, Copper Mountain. The Early Mesozoic deposits formed either during or just after Late Triassic arc formation in the Quesnel and Stikine terranes prior to terrane accretion to continental North America. The younger Late Cretaceous to Eocene calc-alkalic porphyry deposits include Granisle Cu-Au±Mo and Endako Mo. They formed in an intracontinental arc setting after the accretion and assembly of the Cordilleran terranes.

Deposits from both calc-alkalic and alkalic host-rocks and metal assemblage were selected for this study. Highland Valley, Mount Polley, Mount Milligan, Lorraine, Huckleberry and Endako deposits represent examples of the typical styles and assemblages of BC porphyry deposits and therefore were selected for this project (Figure 1).

Highland Valley Cu-Mo porphyry district

The Highland Valley Cu-Mo district in southern BC is the largest cluster of porphyry deposits in the region hosted within the Late Triassic calc-alkaline Guichon Creek batholith (65 × 20 km) which intruded Triassic Nicola Group volcanic and sedimentary rocks (Figure 2;

Casselman et al., 1995). Porphyry centers include Valley, Lornex, Highmont, Alwin, Bethlehem and JA deposits (Figures 2 and 3).

This composite zoned batholith ranges from diorite and quartz diorite at the border to younger granodiorite in the centre. There are three main types of granodiorite that host mineralization at Highland Valley (Figures 3 and 4). Bethsaida phase with composition ranging from quartz-monzonite to granodiorite is characteristics by rounded quartz phenocrysts and abundant coarse biotite and plagioclase phenocrysts (Figure 4a) hosts Valley, Alwin, Highmont and Lornex deposits. Bethlehem phase granodiorite is characterized by lack of quartz phenocrysts and 5-10% hornblende (Figure 4b) and the Guichon granodiorite variety is characterized by abundant (ca. 15%) hornblende phenocrysts (Figure 4c). Bethlehem deposit is hosted largely in Bethlehem phase and Guichon variety but some mineralization occurs in late breccia bodies and porphyry dykes (Figure 4d). Emplacement of the Bethlehem phase and associated mineralization occurred prior to the Bethsaida phase which was associated with the more significant mineralization event (Casselman et al., 1995).

Several stages and styles of alteration and mineralization are identified. At the Alwin mine, mineralization is characterized by narrow, steeply-dipping ore zones that typically contain high-grade ores (Figure 5). At Highland Valley, mineralization is characterized by abundant quartz stockworks and veins (Figures 6 and 7b). At Bethlehem, mineralization is characterized by narrow veins and breccia bodies (Figures 7d and 7f). K-silicate alteration of the Bethsaida granodiorite is characterized by pervasive and veinlet-controlled K-feldspar alteration and recrystalized biotite (Figure 7a). At Bethlehem, remnant of K-silicate alteration is recorded in breccia bodies as fine-grained pervasive biotite (Figure 7d). Much of the sulphide mineralization is, however, associated with overprinting quartz-green muscovite alteration (Figure 7c). The green muscovite alteration occurs in all deposits but it is more abundant in Valley and Alwin mines (Figures 5d, and 7c). Albite, epidote and chlorite alteration assemblage (sodic-calcic alteration?) occurs at Bethlehem (Figure 7e) and commonly lack sulphide mineralization. It is overprinted by white, fine-grained muscovite with lesser chlorite along veinlets (Figure 7f). Late epidote and calcite veins also occur. Further detail of alteration and mineralization can be found in Casselman et al. (1995) and Alva Jimenez (2011).
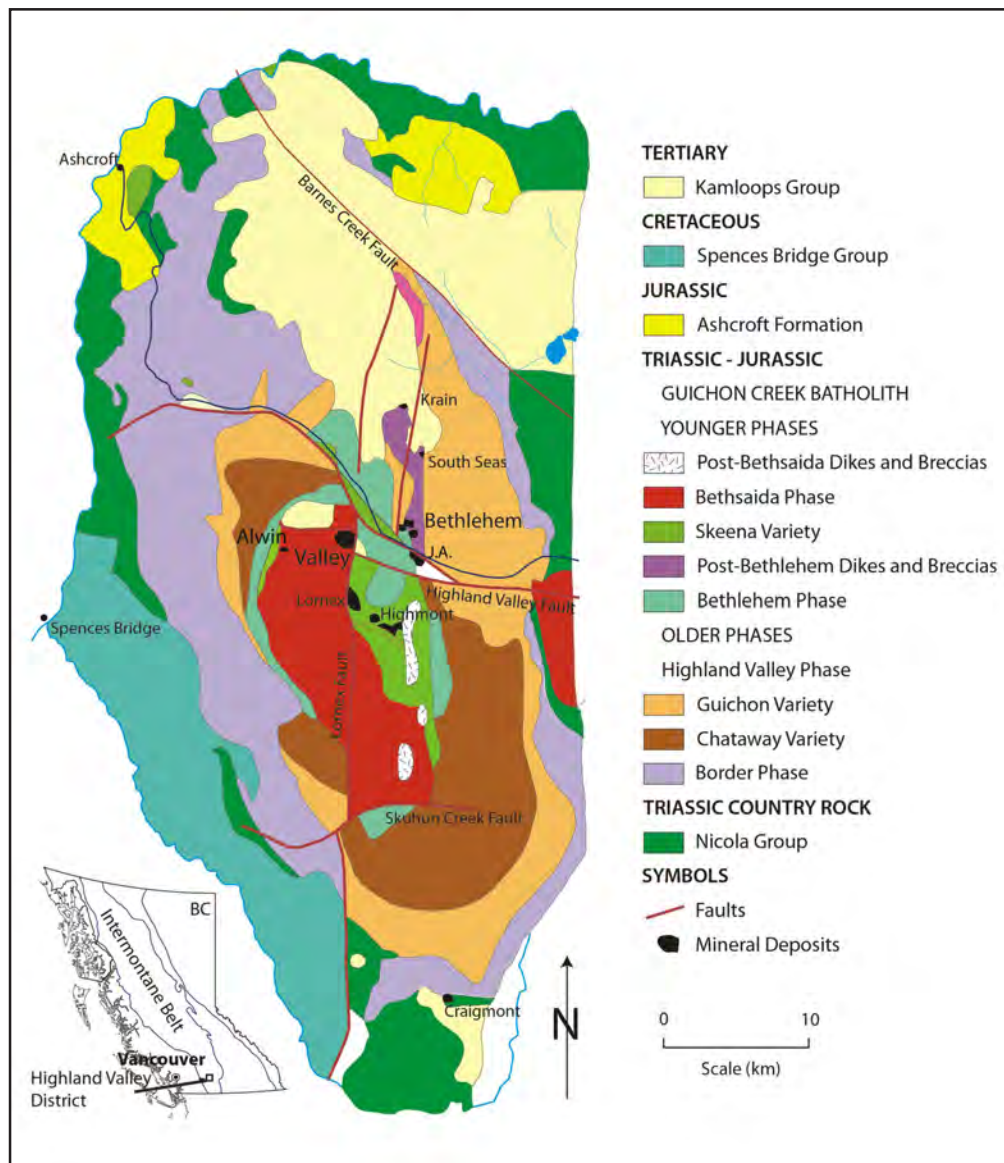
Figure 2: Geological map of the Late Triassic calc-alkaline Guichon Creek batholith showing various intrusive phases that intruded the Triassic sedimentary rocks (redrafted from Casselman et al., 1995).

Figure 3: Aerial photo of the Highland Valley district showing main mineralized centers of Valley, Bethlehem (Huestis, Jersey and Iona pits) and Alwin. Approximate boundaries of main intrusive bodies (Bethsaida, Bethlehem and Guichon) are shown. Aerial photo is courtesy of Teck.

4
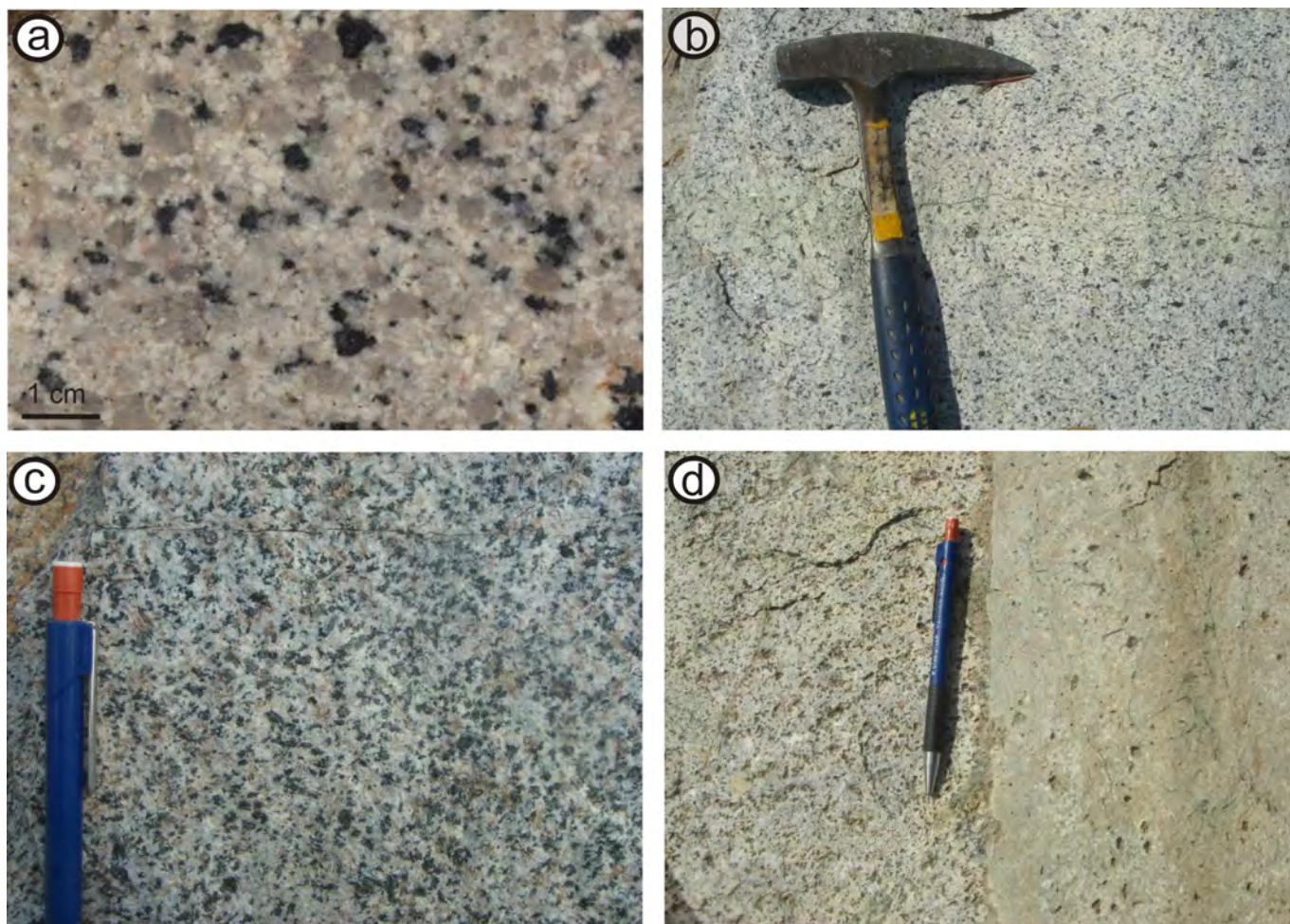
Figure 4: Samples of the fresh host-rocks at Highland Valley: (a) Bethsaida phase with compositions ranging from quartz-monzonite to granodiorite with characteristic rounded quartz phenocrysts and abundant coarse biotite and plagioclase phenocrysts (ALW-5). (b) Bethlehem phase granodiorite characterized by lack of quartz phenocrysts and 5-10% hornblende (BET-1). (c) Guichon granodiorite variety characterized by abundant (ca. 15%) hornblende phenocrysts (BET-14). (d) A late plagioclase porphyry dyke (right) cuts the Bethlehem granodiorite. [numbers in the bracket are sample numbers] .

Mount Polley Cu-Au porphyry deposit

The alkalic Mount Polley Cu-Au deposit is hosted within Triassic–Jurassic diorite-monzonite intrusions and associated breccia bodies. Alteration-mineralization progresses outward from a higher temperature core of biotite to an intermediate actinolite zone and an outer zone of K-feldspar and albite (Fraser et al., 1995; Logan and Mihalynuk, 2005). Copper and gold values are closely correlated with high magnetite concentrations (Deyell and Tosdal, 2005).

Mount Milligan Cu-Au porphyry deposit

The Middle Jurassic Mount Milligan deposits are hosted by three main porphyritic monzonite stocks and adjacent volcanic rocks of the Late Triassic Takla Group. The deposit displays classic zoned alteration-mineralization

of potassic, with a bornite-rich core, surrounded by a pyrite dominated sulphide zone and sodic calcic and propylitic alteration (Sketchley et al., 1995; Jago and Tosdal, 2009).

Lorraine Cu-Au porphyry deposit

Farthest to the north, the Lorraine alkalic Cu-Au porphyry deposit is hosted within the Duckling Creek syenite complex of the Late Triassic–Cretaceous Hogem batholith, which intrudes the Late Triassic Takla Group volcanic and sedimentary sequences (Nixon and Peatfield, 2003). Mineralization occurs in three zones along strike over a distance of approximately 1.5 km within a northwest-trending corridor dominated by syenitic rocks. Mineralization is characterized by finely disseminated Cu-Fe sulphide minerals in fine-grained K-feldspar biotite rock, biotite pyroxenite and syenitic rocks, and lacks

Figure 5: Highland Valley, Alwin mine: (a) Typical narrow, near vertical ore zone trending N70°E, oxidized at the surface. (b) Entrance of one of the old adits. (c) Example of very strong green muscovite alteration and associated chalcopyrite mineralization cutting the host Bethsaida granodiorite (AM-08-04A).

features such as stockwork veining and breccia (Bath and Cooke, 2008). Chalcopyrite and bornite occur as blebs and semi-massive sulphide in pyroxenite (Bishop et al., 1995)

Huckleberry Cu-Mo porphyry deposit

The Huckleberry Cu-Mo porphyry deposit is hosted in Jurassic andesite and dacite volcanic rocks and tuffs of the Telkwa Formation which are intruded by at least two small stocks of Late Cretaceous porphyritic hornblende-biotite-feldspar granodiorite. Mineralization is hosted in both volcanic rocks and granodiorite and is closely associated with strong fine grained biotite-albite alteration (also referred to as hornfelse) with minor K-feldspar, amphibole and chlorite. Sulphide mineralization is associated with quartz veins, with magnetite and purple anhydrite. The central K-silicate alteration grades outward into a chlorite-epidote-pyrite alteration with local carbonate (Jackson and Illerbrun, 1995).

Endako Mo porphyry deposit

The Endako molybdenum deposit is hosted within composite calc-alkaline Endako batholith which is composed of more than twenty distinct plutonic phases ranging in composition from diorite, to gabbro, granodiorite and monzogranite (Whalen et al., 2001). Kimura et al. (1976) interpreted the batholith as consisting of deeper level mafic intrusions located along the margins, broadly changing to felsic, epizonal pluton along a central axis. The Endako molybdenite deposit is located within this central axis. It is hosted in Endako quartz-monzonite which is an equigranular rock with quartz and pale pink to orange K-feldspar phenocrysts and less biotite. This unit is intruded by several pre- and post-mineral dykes.

The most abundant ore-related minerals are molybdenite, pyrite and magnetite, with minor amounts of chalcopyrite. Bulk of the ore is concentrated in the ribbon-textured quartz veins. Three types of hydrothermal alteration occur at the mine. The early stage K-silicate alteration consists of K-feldspar and biotite envelopes on veins and fractures. This is overprinted by quartz-sericite-pyrite assemblage. Pervasive late stage kaolinite alteration has overprinted the host rocks. Although minor ore is associated with K-silicate alteration, much of the molybdenite is related to the sericite alteration associated with ribbon-texture veins (Bysouth and Wong, 1995; Selby et al., 2000; Villeneuve et al., 2001).

Figure 6: Highland Valley, looking northeast from the edge of the Valley pit (active mining) to the Bethlehem deposit (abandoned open pits) during summer of 2009.

MATERIALS AND METHODS

Sampling

Samples were collected from the Highland Valley (33), Mount Milligan (12), Mount Polley (8), Lorraine (13), Huckleberry (7) and Endako (6) deposits (Figure 1). Samples were selected from different alteration assemblages at various locations to determine and characterize the occurrence of resistate minerals at various zones in a porphyry system. Samples were also collected from unmineralized and fresh host-rocks for direct comparison. Samples were commonly collected from mine benches or trenches. Samples from Mt. Milligan were collected from drill holes and sample from Lorraine were from outcrops. Highland Valley was sampled in more detail than other porphyry deposits. Samples from Endako were obtained from another Mineral Deposit Research Unit (MDRU) project (Dianne Mitchinson, pers. comm. 2010). Lorraine samples were retrieved from the archive of a previous study within the MDRU-CODES collaborative Alkalic deposits study (Bath and Cooke, 2008). Appendix 1 provides list of all samples, location and a short field description.

Methods

An integrated analytical technique was employed at MDRU to establish the most valid and cost effective mechanism for characterizing PIMS. Analytical work includes a petrographic study employing optical and cathodoluminescence (CL) microscopy and scanning electron microscopy (SEM) to characterize the abundance and physical properties of various indicator minerals, including shape, size, colour and luminescence. Selected grains were analyzed by electron microprobe for their trace-element composition to test whether there are key chemical features in the PIMS that are unique to mineralized porphyry copper deposits.

Cathodoluminescence Microscopy: A Cambridge Image Technology Ltd MK 4A model cold cathodoluminescence stage mounted on a petrographic microscope was used to study the internal textures of the apatite grains. The samples were irradiated in a vacuum chamber with an electron beam of approximately 15 kV and the current set at 350–500 μA.

Electron-probe micro-analyses: Electron-probe micro-analyses of apatite were done on a fully automated CAMECA SX-50 instrument, operating in the wavelength-dispersion mode with the following operating conditions: excitation voltage, 15 kV; beam current, 10 nA; peak count time, 20 s (40 s for F, Cl); background count-time, 10 s (20 s for F, Cl); spot diameter of 10 μm. For the elements considered, the following standards, X-ray lines
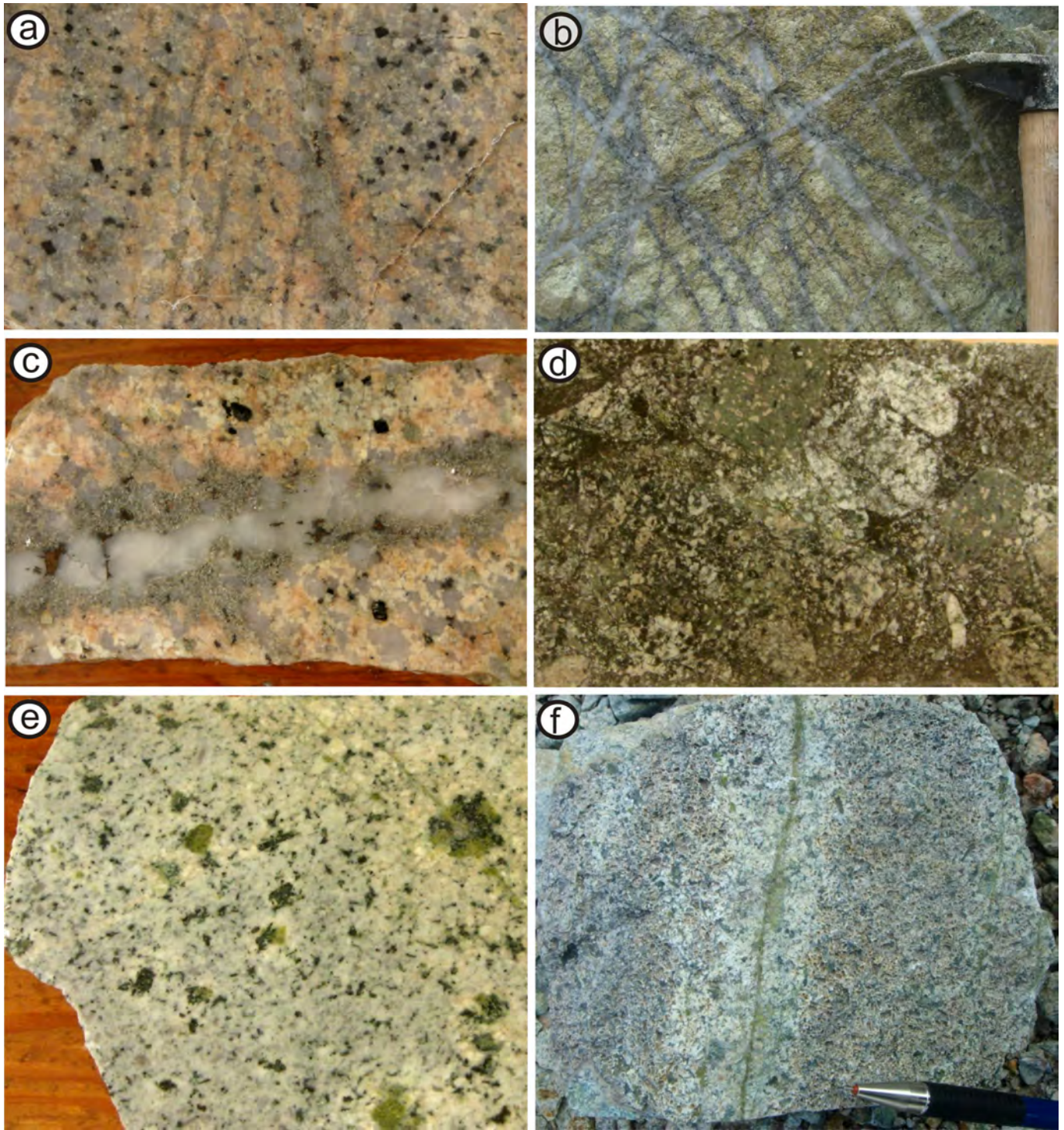
Figure 7: Examples of common alteration types at Highland Valley: (a) K-silicate alteration of the Bethsaida granodiorite characterized by pervasive and veinlet-controlled K-feldspar alteration and re-crystalized biotite, Valley pit (HLV-3a). (b) Typical quartz-sulphide stockwork and associated green muscovite alteration, Valley pit. (c) An example of quartz-chalcopyrite-bornite vein with coarse green muscovite halo overprinting earlier K-feldspar alteration, Valley pit (HLV-3b). (d) Breccia body from Iona pit, Bethlehem mine, containing clasts of Bethlehem phase and plagioclase porphyry with strong pervasive biotite alteration (BET-17). (e) Bethlehem granodiorite with pervasive sodic plagioclase alteration and abundant epidote, Bethlehem mine (BET-8). (f) Bethlehem granodiorite is cut by a sericite vein (white color) and a late epidote veinlet, Bethlehem mine (BET-4).

and crystals were used: albite, Na$K\alpha$, TAP; kyanite, Al$K\alpha$, TAP; diopside, Mg$K\alpha$, TAP; apatite, P$K\alpha$, TAP; apatite, Ca$K\alpha$, PET; barite, S$K\alpha$, PET; synthetic rhodonite, Mn$K\alpha$, LIF; SrTiO$_3$, Sr$L\alpha$, TAP, topas, F$K\alpha$, TAP; scapolite, Cl$K\alpha$, PET. Data reduction was done using the 'PAP' $\phi(\rho Z)$ method (Pouchou & Pichoir 1985).

INDICATOR MINERALS IN PORPHYRY COPPER DEPOSITS

Indicator minerals are defined as minerals which are: 1) chemically stable in weathered environments (i.e., resistate); 2) heavy, so that they may be easily concentrated; 3) sufficiently coarse grained to be readily identified (Averill, 2007); and 4) display characteristic features that link them to a specific type of mineralization (McClenaghan, 2005). Coarse, heavy resistate minerals have long been known to occur in porphyry copper deposits, both in host intrusions and as hydrothermal alteration products (e.g., Schwartz, 1953, Gustafson and Hunt, 1975, Lang et al., 1995). However, characteristic features that link these minerals to porphyry copper mineralization are not well known.

Resistate minerals can record salient features of the porphyry system from early magmatic (e.g., zircon) to late hydrothermal (e.g., apatite) and subsequent supergene oxidation stages. Thus, when formed or altered by hydrothermal fluids characteristic of the mineralizing porphyry environments, the physical properties of these minerals may change such that they display unique colour, size and shape characteristics, which allows there characterization as an indicator mineral and use as a prospecting tool.

Early work on heavy accessory minerals in porphyry copper deposits mainly focused on the economic exploitation of these minerals (e.g., Czamanske et al., 1981), however, several studies noted the unique physical and chemical features of the resistate minerals associated with various stages of hydrothermal alteration in porphyry copper deposits (Table 1). More recently, chemical and physical properties of apatite and rutile were the subject of studies showing the overall evolution of the hydrothermal system (e.g., Streck and Dilles, 1998; Scott, 2005).

Apatite, rutile, zircon, titanite, monazite and garnet are resistate minerals that may be commonly associated with calc-alkaline and alkaline porphyry deposits (Table 1). Tourmaline, dumortierite, andalusite, diaspore and quartz commonly occur with calc-alkaline porphyry deposits. Ore sulphide minerals and iron oxides such as magnetite are unstable in the weathering environment and are generally not, or are poorly preserved in surficial sediments. However, these minerals survive in some weathering environment or can be converted to new stable mineral or assemblage in certain hypogene or supergene environment such as jarosite, thus making them suitable for use as indicator phase (see below). Table 1 summarizes key characteristics of the common resistate minerals in porphyry copper deposits.

Apatite

Apatite (Ca$_5$(PO$_4$)$_3$F,OH,Cl) is a common accessory mineral occurring in various host-rocks and K-silicate alteration associated with mineral deposits. Apatite structure can incorporate a wide range of transition metal, REE and anion impurity which can be used as marker to evaluate chemical condition of rock formation or associated hydrothermal alteration. Some of common substitutions occurring in apatite are (Waychunas, 2002):

Sr^{2+}, Mn^{2+}, Fe^{2+}, REE, Y^{3+}, Na^+ $\leftrightarrow$ Ca^{2+} site
Si^{4+}, As^{5+}, S^{6+} and C^{4+} $\leftrightarrow$ P^{5+} site
Cl^- and OH^- $\leftrightarrow$ F^-
$2Ca^{2+}$ $\leftrightarrow$ $Na^+ + REE^{3+}$
$Ca^{2+} + P^{5+}$ $\leftrightarrow$ $REE^{3+} + Si^{4+}$

Luminescence is one property of apatite caused by trace element activators substitutions. Thus, Mariano (1988) and Kempe and Götze (2002) have shown that apatite from mineralization related to alkaline rocks exhibits blue and violet cathodoluminescence (CL) due to activation by trace quantities of rare earth element ions (Ce^{3+}, Eu^{2+}, Sm^{3+}, Dy^{3+} and Nd^{3+}), whereas those from P-rich granite show strong Mn^{2+}-activated yellow-greenish luminescence.

Williams and Cesbron (1977) noted that apatite of porphyry copper origin displays a characteristic bright orange colour under UV light, and shows a complicated history of corrosion and redeposition with characteristic zoning (Liesegang rings). The rings can often be detected up to 600–1000 m laterally away from the intrusion. The composition of these textures is not well known but they may have recorded changes of the hydrothermal system through time and thus have the potential to provide clues to the productivity of the system.

Trace element compositions of apatite have been used to recognize the host-rock and degree of fractionation, as well as the oxidation state of the magma (Tepper and Kuehner, 1999; Belousova et al., 2002). Studies on apatite at Yerington batholith, Nevada (Streck and Dilles, 1998) and

Table1: Characteristics of resistate minerals occurring in BC porphyry copper deposits (D = density, PCD = porphyry copper deposits).

Mineral	D	Occurrence in PCD	Characteristic features in porphyry deposits	south-central BC example	Selected References
Rutile	4.2	Occurs in potassic and phyllic zones as alteration product of biotite, ilmenite, titanomagnetite, titanite and amphibole.	Red color due to high copper content; crystal length:width ratio increases outward the deposit; grains proximal to the mineralized center are larger and zoned; abundance and grain size follows the Cu grade; high concentration of V, Ta and Sc; Cr+V:Nb+Ta is high; V-Sb-W-rich rutile defines the Au-rich zone.	Mt. Milligan, Babine Lake, Highland Valley	Williams and Cesbron, 1977; Desborough and Sharp, 1978; Czamanske et al., 1981; Harris, 1989; Nelson and Bellefontaine, 1996; Scott, 2005; Rabbia et al, 2009
Apatite	3.2	Occurs in hostrock and with early potassic alteration but records a history of dissolution and precipitation during subsequent alterations.	Fluoresce bright orange color in the UV; shows complicated history of corrosion and redeposition with a characteristic zoning (Liesegang rings); rings can often be detected 600-1000 m laterally away from the intrusive; commonly displays sulphur-rich cores abruptly changing to sulphur-poor rims; it is chlorine-rich.	Mt. Polley, Galore Creek, Lorraine, Granisle, Highland Valley	Carson and Jambor, 1974; Williams and Cesbron, 1977; Streck and Dilles, 1998; Tepper and Kuehner, 1999; Belousova et al., 2002; Kempe and Götze, 2002; Bath et al., 2006; Liaghat and Tosdal, 2008
Garnet	~3.9	Occurs in the periphery of porphyry deposits	Displays zoning, dissolution and change in composition. Ti-rich andradite commonly reported; hydrothermal titanian andradite can have as much Ti-Si as igneous varieties, but has zero or negative amounts of $TiMg[Fe^{3+}]_{-2}$	Mt. Polley, Galore Creek, Lorraine	Watson, 1969; Russell et al., 1999; Nixon and Peatfiled, 2003; Micko 2010
Zircon	4.6	Commonly magmatic, occurring with the host intrusion but few studies report distinct hydrothermal zircon hosted in hydrothermal veins.	Rose zircon commonly reported; hydrothermal, spongy, inclusion-rich zircon may show complex internal textures in which secondary domains cut across primary growth zones; porphyry copper deposits are associated with intrusions with zircon having Ce(IV)/Ce(III)>300 and EuN/EuN*>0.4	Mt. Milligan, Mt. Polley, Ajax	Mortensen et al., 1995; Nelson and Bellefontaine, 1996; Ballard et al., 2002; Hoskin, 2005; Pettke et al., 2005; Schaltegger, 2007
Monazite	~5.1	Commonly magmatic occurring with the host intrusion	Hydrothermal monazite is characterized by its low ThO_2 content (0–1 wt %) and is distinct from that of igneous monazite (3 to >5 wt %).	Endako	Schand and Gorton, 2004; Villeneuve et al., 2001
Titanite	~3.5	Commonly magmatic occurring with the host intrusion	Blond titanite reported. Composition of zoned titanite is used to examine, magma oxidation state and mixing and compatibility of Mo and W in felsic intrusions. Secondary titanite rims on magnetite contain higher Cr, Zn and Mo, and lower REE, relative to magmatic titanite.	Mt. Milligan; Mt. Polley; Copper Mountain	Nakada, 1991; Mortensen et al., 1995; Nelson and Bellefontaine, 1996; Piccolie et al., 2000
Tourmaline	~3	Commonly with transitional phyllic or breccia bodies.	Dravite is more common; associated with or without mineralization.	Megabuck, Highland Valley	Panteleyev et al., 1996; Slack, 1996
Jarosite	~3	Supergene oxidation	May occur with goethite and/or copper oxides	Mt. Milligan	
Magnetite	5.1	Magmatic and associated with K-silicate alteration	Can form resistate phase especially when aggregated with rutile, titanite and quartz. Hydrothermal magnetite has less Ti than magmatic magnetite. Geochemistry of magnetite is used to discriminate Fe-oxide occurring in various deposit types.	Mt. Polley; Mt. Milligan; Highland Valley	Arancibia and Clark, 1996; Dupuis and Beaudoin, 2011

Galore Creek porphyry Cu-Au deposit, British Columbia (Liaghat and Tosdal, 2008) demonstrated that zoned apatites have sulphur-rich cores which abruptly change to sulphur-poor rims, indicating that early sulphate-rich magma evolved to sulphate-poor magma via crystallization of anhydrite. Similarly, Bath et al. (2006) demonstrated that apatite crystals from Mount Polley, British Columbia, show fractured inclusion-rich cores and fracture-free inclusion-poor rims with cores enriched in sulphur (4000–5500 ppm) compared to crystal rims (2000–3500 ppm). The decrease in the solubility of sulphur into apatite was attributed to the fluids/melt becoming more reduced; decrease in pressure; increase in temperature; and/or decrease of sulphur within the melt/fluids (Bath et al., 2006). Moreover, apatite associated with porphyry copper deposits are commonly Cl-rich (e.g., Roegge et al., 1974). Thus, apatite can be used as a record for chloride content of the crystalizing melt which may have played a key role in transporting copper (Holland, 1972).

Rutile

Rutile is a ubiquitous accessory mineral in porphyry copper deposits and even its potential as a minable commodity for titanium has been suggested (Williams and Cesbron, 1977; Czamanske et al., 1981). Rutile forms commonly as a result of alteration of Ti-bearing minerals. Because Ti is relatively immobile element, rutile grade represents Ti content of the original host-rock. However, type of alteration is more important to the rutile concentration than the Ti-content of the original host-rock. There are several ways to form rutile in porphyry copper deposits:

1. Alteration of primary magmatic biotite (Ti-rich) to secondary hydrothermal biotite (Ti-poor) (e.g., Moore and Czamanske, 1973). Titanium liberated by recrystallization of biotite forms rutile in, or adjacent to, secondary biotite. This rutile ranges from microscopic (sagenitic) needles commonly with reticulated pattern, through fine crystals, to crystals as coarse as 0.25×0.5mm (Czamanske et al., 1981). The controls on proportion of coarse to needle rutile is not known but it is probably influenced by overall alteration history.
2. Alteration of biotite to chlorite: This is texturally similar to the rutile formed with secondary biotite.
3. Alteration of amphibole to biotite or chlorite: Amphiboles are typically recrystallize or replaced to varieties with lesser TiO_2 content (Carson and Jambor,

1974). However, amphiboles commonly contain only one-fourth as much TiO_2 as coexisting biotite (Czamanske et al., 1981).
4. Alteration of titanite: Titanite (sphene) may break down to form rutile, carbonate and quartz. These minerals commonly form a mosaic assemblage which preserves the original form of the wedge-shaped titanite crystal.
5. Alteration of ilmenite or titaniferous magnetite: Rutile can form after oxidation of ilmenite or titaniferous magnetite to hematite.

Therefore, rutile occurs in various alteration zones in porphyry copper deposits such as potassic, phyllic and even inner fringes of prophylitic zones. More importantly, it displays physical and chemical characteristics that can be used for explorations. For example, crystal length:width ratio increases outward the deposit (Williams and Cesbron, 1977) and grains proximal to the mineralized center are reported to be larger and zoned (Scott, 2005). Czamanski et al. (1981) suggest that the abundance and grain size of rutile follow the Cu grade. The characteristic red color of the rutile in thin section is attributed to a high copper content of 100-500 ppm (Williams and Cesbron, 1977). Such rutiles also have high ratio of Cr+V:Nb+Ta.

Vanadium, tantalum and scandium are common trace elements in rutile and their concentration can be used to discriminate porphyry-related rutile and the proximity to the mineralization. Thus, vanadium-rich rutile occurs proximal to the core of porphyry deposit (Desborough and Sharp, 1978; Scott, 2005). Rabbia et al. (2009) documented the reverse relationship between Mo content of rutile and ore grade at El Teniente porphyry Cu-Mo deposit, Chile. They show low temperatures (400–550°C), Mo-poor rutile (5.4±1.1 ppm) is dominantly in the mafic wallrocks (high-grade ore), while high-temperature (550-700°C), Mo-rich rutile (186±20 ppm) is found in the Mo-poor felsic porphyries (low-grade ore). Thus, the high-temperature (>550°C), oxidized and low $a(H_2S)$ hydrothermal fluids delayed or suppressed sulphide precipitation to temperatures below 550°C, enhancing Mo partitioning into high-temperature rutile.

Zircon

Zircon occurs in most calc-alkaline intrusions and is resistant to subsolidus alteration. Trace element composition of zircon has been used to discriminate fertile intrusive body. Thus, Ballard et al. (2002) in a study of barren and mineralized intrusive bodies in northern

Chile demonstrated that porphyry copper mineralization is directly associated only with intrusions with zircon Ce(IV)/Ce(III)>300 and EuN/EuN*>0.4 reflecting oxidation states of magma. Moreover, there are reports that zircon may have precipitated from a hydrothermal fluid or a fluid-saturated residual melt (Schaltegger, 2007). Such zircons at the Boggy Plain zoned pluton, eastern Australia, are characterized by higher concentration of all measured trace-elements relative to magmatic zircon in the same rock (Hoskin, 2005). Zircon in porphyry copper deposits displays distinctive rose color and some are colorless (Averill, 2007) but the cause of color variation and its relationship to the mineralization is not studied.

Tourmaline

Tourmaline is a common constituent of a wide range of hydrothermal ore deposits (Slack, 1996) and particularly occurs with granitoid-related breccia pipes and porphyry copper deposits (e.g., Sillitoe and Sawkins, 1971). These breccia pipes are typically barren of economic mineralization but some contain significant copper mineralization, such as at Los Bronces-Rio Blanco (Warnaars et al., 1985). Moreover, non-breccia tourmaline veins occur commonly in porphyry deposits both during the main- (e.g., El Teniente) and post-main stages (e.g., El Salvador) of mineralizations (Clark, 1993). Therefore, the application of tourmaline for exploration is always challenged because of its wide spectrum of occurrences. To our knowledge, there has been no study to discriminate between ore related and barren tourmaline in porphyry deposits. However, Ethier and Campbell (1977) and Slack (1982) documented the preferential occurrence of Mg-rich tourmaline with massive sulphide deposits. Moreover, Taylor and Slack (1984) identified anomalous concentration of Cr, Cu, Pb, Sr, and V in tourmaline from massive sulphide deposits.

Andalusite, diaspore and corundum

Andalusite, diaspore and corundum commonly occur in shallow-level advanced argillic alteration zones of porphyry deposits replacing muscovite and clay minerals (Watanabe and Hedenquist, 2001; Bouzari and Clark, 2006). However, andalusite is a common mineral in metamorphic terrains and diaspore forms a major component of bauxite. Therefore, these aluminum-rich minerals have no exploration use in such terrains unless the hydrothermally originated grains can be discriminated.

Quartz

Quartz is by far the most abundant resistate mineral in porphyry copper deposits but it is not considered as a workable indicator mineral because it most commonly occurs in large amount in the light mineral fraction. However, in certain areas, especially in terranes with non-transported overburden, examination of light mineral fraction may provide clues on the mineralization.

Recognition of the "porphyry style" quartz veins in weathered and eroded outcrops has played a significant role in exploration of major porphyry copper deposits (e.g., El Salvador, Chile: Gustafson and Hunt, 1975). Hydrothermal quartz is characterized by abundant fluid inclusions and cathodoluminescence features that reflect physical and chemical conditions of quartz precipitation. Rusk et al. (2006) demonstrated that CL intensity of quartz increases by Ti concentration which, in turn, is controlled by temperature of quartz precipitation. The upward decrease of high-density fluid inclusions from potassic to advanced argillic zones (e.g., Hedenquist et al., 1998; Bouzari and Clark, 2006) may provide clues on the erosion level of a buried deposit and potential of exploration at depth.

Sulphide and iron-oxide minerals

Sulphide and iron-oxide minerals are not stable under the oxidizing conditions of surficial environments therefore do not ultimately survive weathering processes. However, iron oxide minerals in particular, and lesser sulphides are commonly found in unweathered glacial sediments (e.g., Plouffe et al., 2006), particularly if pre-glacial supergene oxidation was not a dominant feature. In BC, multiple glaciations ensured that fresh rocks were exposed to erosion during the youngest glacial event so sulphide and iron oxide minerals occur locally in unweathered glacial sediments below the post-glacial soil weathering zones. Supergene oxidation processes can also convert hypogene sulphide minerals into stable, insoluble minerals such as jarosite and turquoise, which can also be used as PIMS. Similarly, magnetite is not stable in supergene oxidation environment but will convert to a mixture of hematite and rutile which are more resistate.

TEXTURAL CHARACTERISTICS

Petrographic observations indicate that apatite, zircon, rutile and titanite are common resistate minerals in the studied deposits. Magnetite is associated with

titanite, rutile and hematite and also displays distinctive characteristics. Both apatite and the Fe-Ti oxide phases are by far the most common resistate minerals occurring across the wide range of host-rocks and alteration assemblages. More critically, the physical and chemical properties of these minerals are significantly different in mineralized/ altered rocks compared to fresh host-rocks. The textural properties of apatite and magnetite presented in this report are based largely on observations from Highland Valley and comparisons are made with observations from several other BC porphyry deposits.

Apatite

Apatite occurs in all studied deposits but it is rarely documented as an accessory mineral associated with alteration assemblages. Samples of apatite from fresh or least altered host-rock are compared with apatite associated with various alteration assemblages. Apatite commonly displays euhedral crystal shape and its hexagonal form is distinctive. However, small apatite grains surrounded by quartz or feldspar are difficult to recognize under optical microscope. Observations and descriptions of apatite textures are largely based on its luminescence properties because apatite commonly appears uniform if examined under the optical petrographic microscope or even SEM. However, zones with abundant inclusions in apatite are better observed under optical microscope.

Apatite in the Highland Valley Cu-Mo porphyry deposit

Apatite is a common accessory mineral in most granitoid rocks and is common in unaltered Guichon and Bethlehem granodiorite host rocks. Apatite also occurs with K-silicate alteration especially in the Valley deposit and displays unique characteristics occurring with phyllic alteration.

Apatite in fresh host-rock: Apatite in fresh granodiorite occurs as euhedral grains 100 to 200 µm in diameter. Smaller grains (<10 µm) sometimes occur as inclusions in other minerals such as in magnetite (Figure 8a). These apatite grains mostly show no major internal structures when examined by CL or SEM. Under CL, all apatites in fresh granodiorite display strong luminescence of yellow to yellow-green (Figure 8a and 8b). The yellow luminescence is attributed to excitation by Mn^{2+} (Mariano, 1988; Waychunas, 2002). However, some fresh apatite grains display zoning with yellow-brown luminescence with brown luminescence occurs at the core of apatite

(Figure 8c) or as narrow zone near the rim (Figures 8c and 8d). Zoning in apatite has been considered to be an indicator of magmatic processes such as magma mixing, fractionation and crystallization which are processes that are considered favourable for the formation of porphyry copper mineralization.

Apatite occurring with K-silicate alteration: Apatite in altered granodiorite looks very similar to that occurring with unaltered granodiorite when examined using a polarizing microscope and SEM (Figures 9a and 9b). However, CL microscopy reveals that apatite occurring with K-silicate-altered host-rocks displays a unique green luminescence, probably reflecting Fe^{2+} excitation. The green luminescence occurs at the crystal rim and along fractures in weakly altered apatite (Figure 9b) and as replacements of the entire grain in strongly-altered samples (see below).

Apatite occurring with green muscovite alteration: Apatite occurring with green muscovite alteration and sulphide mineralization (Figure 10a) displays distinct grey luminescence replacing green luminescent phases (Figure 10b). The green luminescence is interpreted to be a remnant of the apatite of the K-silicate alteration. The grey luminescence clearly cuts the green luminescent phase (Figure 10b) indicating its formation after the green luminescent phase. However, figure 10b shows that a narrow rim of green-brown apatite phase has mantled both green and grey apatite phase. This plausibly suggests that K-silicate apatite formed after muscovite-related apatite. Such relationships have rarely been observed in porphyry systems, and therefore may have occurred only locally. Apatite occurring with intense pervasive muscovite alteration (Figure 10d) is intensely replaced by grey luminescence phase producing a "messy" texture (Figure 10e) with zones and bodies of green-grey to dark grey-luminescent apatite. Luminescence zoning on both sides of a micro-fracture hosting chalcopyrite and cutting through apatite grain (Figure 10f) is evidence of a fluid pathway that altered apatite grain.

Apatite in other porphyry deposits

Apatite is also a common mineral in alkalic Cu-Au and calc-alkalic Mo deposits. At Mt. Polley, fresh monzonitic host-rocks have apatites with zoned yellow-brown luminescence with more brownish phases occurring in the core, or as one or two narrow zones in the middle or at the rim of the apatite crystal (Figure 11a). Apatite occurring with K-feldspar and magnetite alteration at Mt. Polley
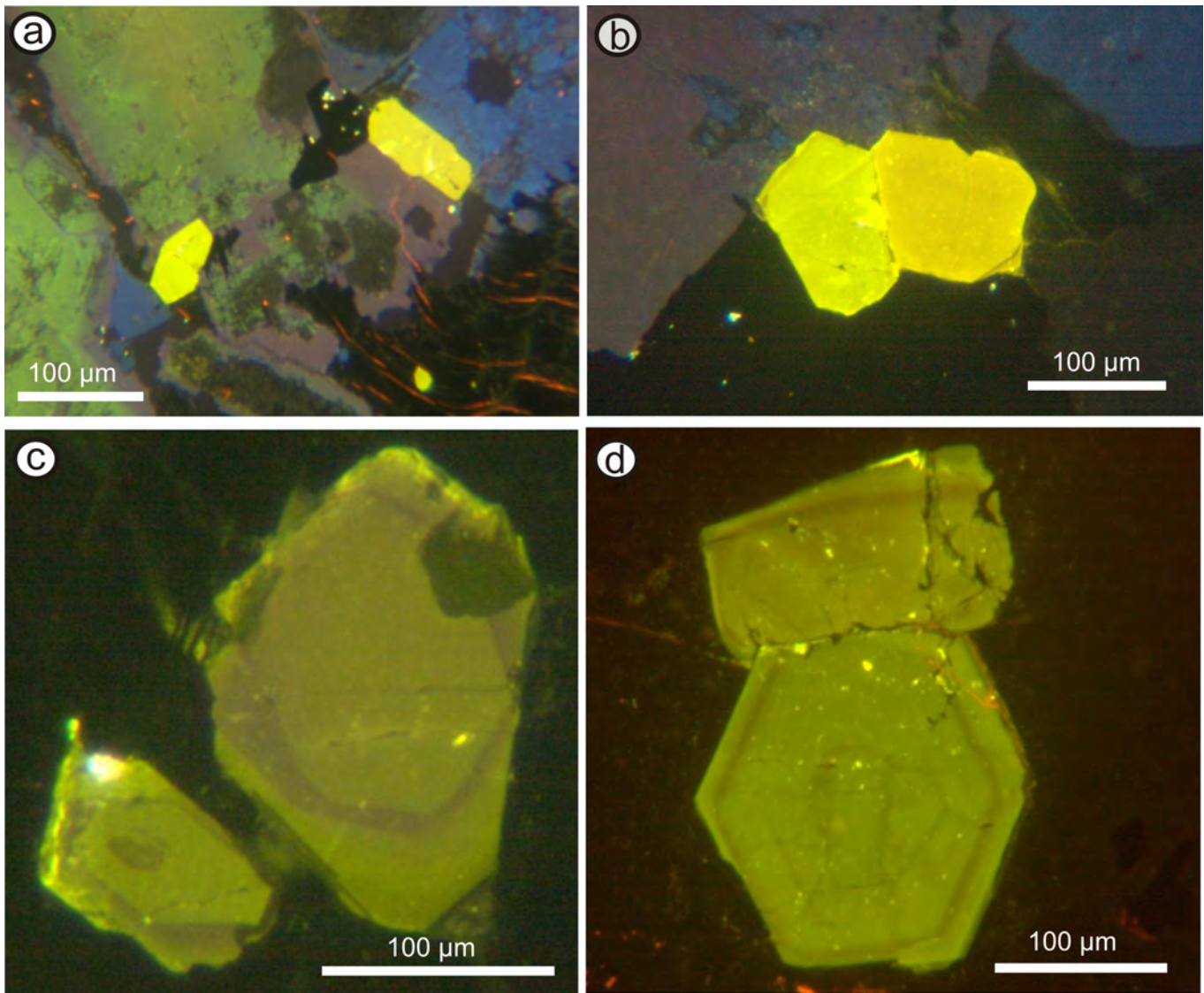
Figure 8: Cathodoluminescence images of Highland Valley apatites from fresh or least-altered host-rock: (a) Sample of fresh Bethsaida granodiorite hosting two large grains of apatite with yellow luminescence surrounded by calcic plagioclase (green), K-feldspar (blue) and magnetite (black). Weak orange rim of calcic plagioclase is probably due to weak alteration (illite?) and red spots are late calcite (AM-08-06). (b) Two grains of apatite with uniform yellow and yellow-pale-green luminescence surrounded by calcic plagioclase (green luminescence), Bethsaida granodiorite (ALW-5). (c) Apatite grains in fresh Bethlehem granodiorite displaying a yellow-brown core and a distinct brown zone (BET-1). Apatite from weakly altered Bethsaida granodiorite displaying yellow-green luminescence and a narrow brown zone near the rim (ALW-7).

shows green luminescence either replacing or overgrowing brown-luminescent apatite (Figure 11b).

Thus, the very bright yellow luminescence of apatite observed at Highland Valley is not common at Mt. Polley. But instead apatite displays yellow-brown to brown luminescence. Apatite occurring with K-silicate alteration at Mt. Polley is similar to that observed in K-silicate altered rock at Highland Valley. Similar relationships were noted for apatite associated with fresh and K-silicate altered rocks at Lorraine and Mt. Milligan.

Apatite occurring with the least-altered granodiorite host-rock at Huckleberry displays yellow-brown to orange-brown luminescence commonly with fine-zoning (Figure 11c). Apatite occurring with biotite-albite alteration at Huckleberry displays abundant green-luminescent phases. However, unlike simple replacement or overgrowth of green-luminescent phase, the K-silicate altered apatite at Huckleberry displays a complex texture of bodies of green-luminescent apatite (Figure 11d). The occurrence, abundance and intensity of green-luminescent apatite, however, correlates with the intensity of the biotite-alteration.
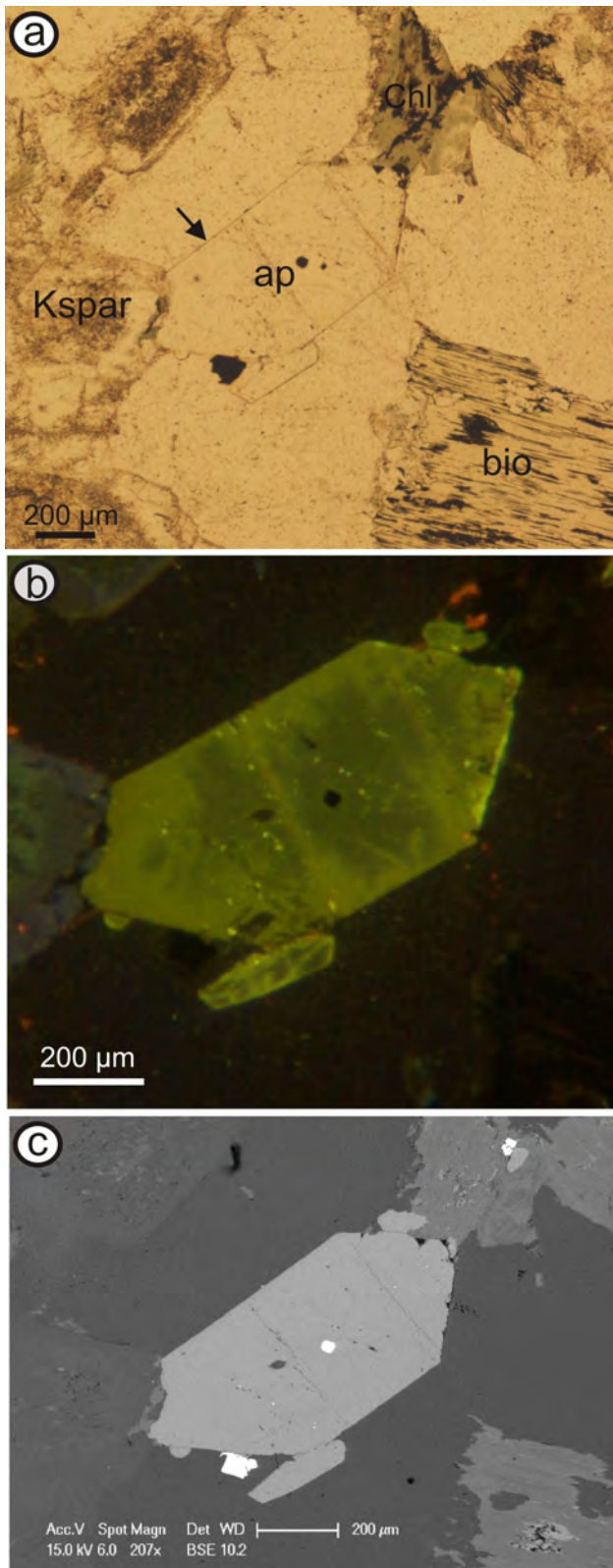
Figure 9: Highland Valley apatite occurring with K-silicate alteration: (a) Plane- polarized photomicrograph showing apatite crystal surrounded by quartz and K-feldspar and weakly altered biotite and minor sulphide. (b) Cathodoluminescence image of the same apatite grain showing the dull yellow-brown apatite is replaced by brighter green luminescent phase at the rims and along fractures. (c) SEM image of the same apatite grain showing no internal structure.

Samples of fresh quartz monzonite host-rocks from the Endako molybdenite deposit were not available, but examination of the least-altered host-rocks identifies zoned apatite with brown luminescence core and green rim (Figure 11e). The perfect zoning between brown and green luminescent phases is different from the typically irregular replacement or overgrowth textures of green luminescence observed at Highland Valley and elsewhere. Endako apatites occurring with K-feldspar alteration display dominantly green luminescence with remnants of brown-green luminescent apatite (Figure 11f).

Therefore, even though most of the molybdenite mineralization formed with overprinting sericite alteration, the apatites occurring with K-silicate alteration at Endako Mo porphyry are texturally similar to those occurring with K-silicate alteration in other porphyry types in BC. However, the zoning relationship between green and brown luminescent apatite in least altered host-rock at Endako suggests that some of the green luminescent phases may have formed during late stage crystallization of K-rich melts and not necessarily during subsequent K-silicate alteration processes.

Magnetite

Magnetite is a common accessory igneous mineral occurring within the granitoid host-rocks of porphyry Cu-Au deposits (magnetite series) whereas ilmenite-bearing granitoid rocks (ilmenite series) are associated with Sn and W mineralization (Ishihara, 1981). Magnetite also occurs in the higher temperature, early stages of hydrothermal alteration in porphyry deposits both before and with K-silicate alteration. Early magnetite-amphibole-plagioclase alteration-mineralization occurs in the Island Copper porphyry Cu-Au-Mo deposit in British Columbia for example, which largely formed prior to the K-silicate alteration and sulphide mineralization (Arancibia and Clark, 1996). Similar magnetite-bearing alteration facies have been described from the Tanama porphyry Cu-Au, Puerto Rico (Cox, 1985), Park Premier Cu-Au-Mo porphyry Utah (John, 1989) and El Galeno porphyry Cu-Mo-Au, Peru (Bouzari, unpublished). Hydrothermal magnetite, averaging 3 to 10 volume percent, also occurs in many K-silicate zones as veinlets or disseminated grains and grain aggregates (Sillitoe, 2000) such as in El Salvador, Chile, in which abundant magnetite, and locally hematite, and titanite (replaced by rutile and hematite) occurs in the deeper part of the K-silicate alteration zone (Gustafson and Hunt, 1975).

Hydrothermal magnetite can be distinguished from
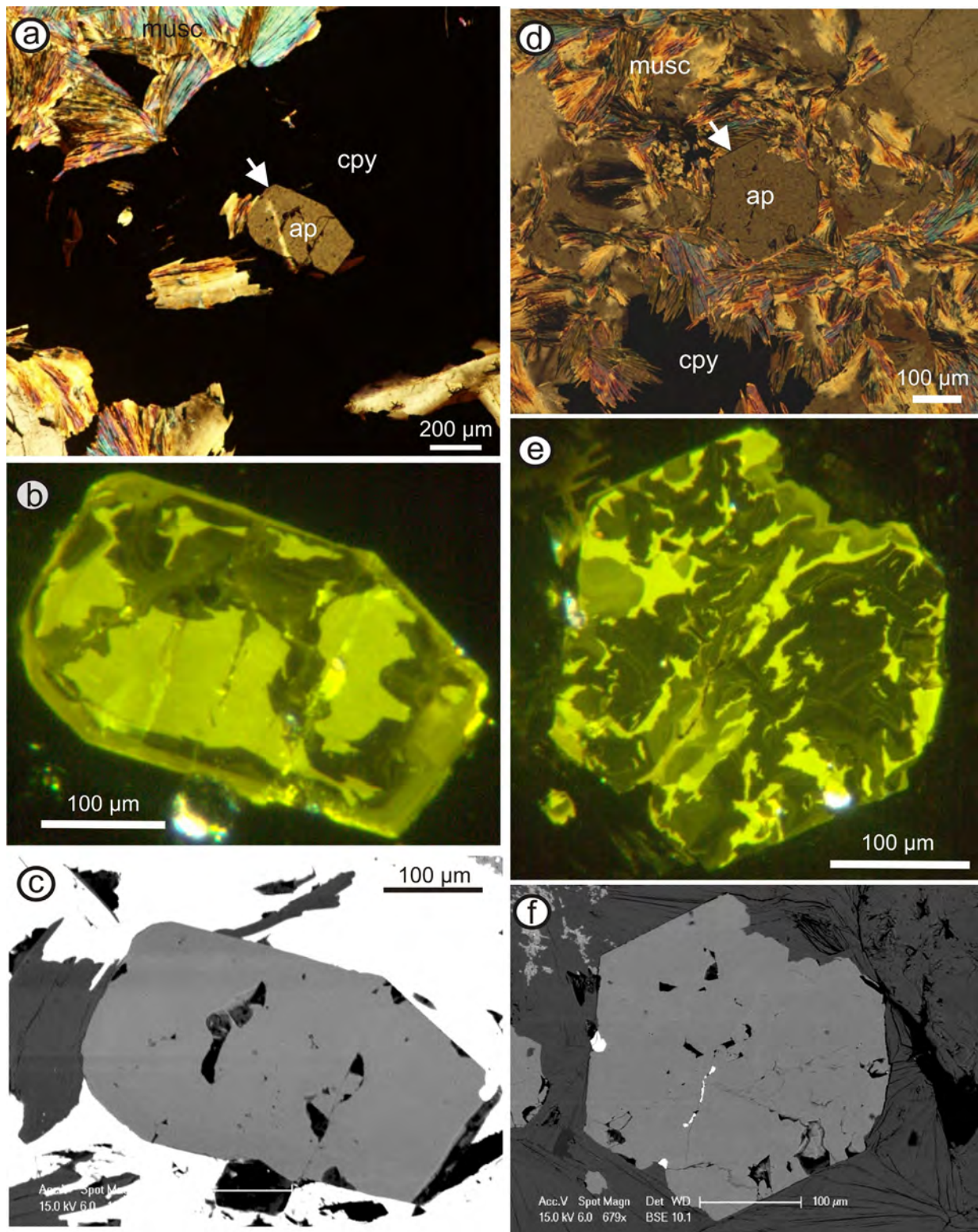
Figure 10: Highland Valley apatites occurring with phyllic (muscovite) alteration: (a) Cross-polarized photomicrograph of apatite occurring with a vein related muscovite and chalcopyrite mineralization (ALW-3). (b) Cathodoluminescence of the same above apatite grain showing an early bright green luminescent phase cut by dull grey luminescent phase. Note that thin green-brown phase has formed at the rim presumably after the grey phase. (c) SEM image of the same above apatite grain. (d) Cross-polarized photomicrograph showing apatite occurring with abundant pervasive coarse muscovite (musc) and chalcopyrite (cpy) mineralization (ALW-8). (e) Cathodoluminescence of the same apatite grain as in (d) showing that a bright green luminescent phase is replaced by a variety of duller grey luminescent phases with fine zoning pattern. (f) SEM image of the above apatite grain showing only weak internal texture–the very bright phase at the rim and inside the apatite is chalcopyrite, which has formed within a micro-fracture that has an envelope of green to grey-luminescent apatite (see above figure).
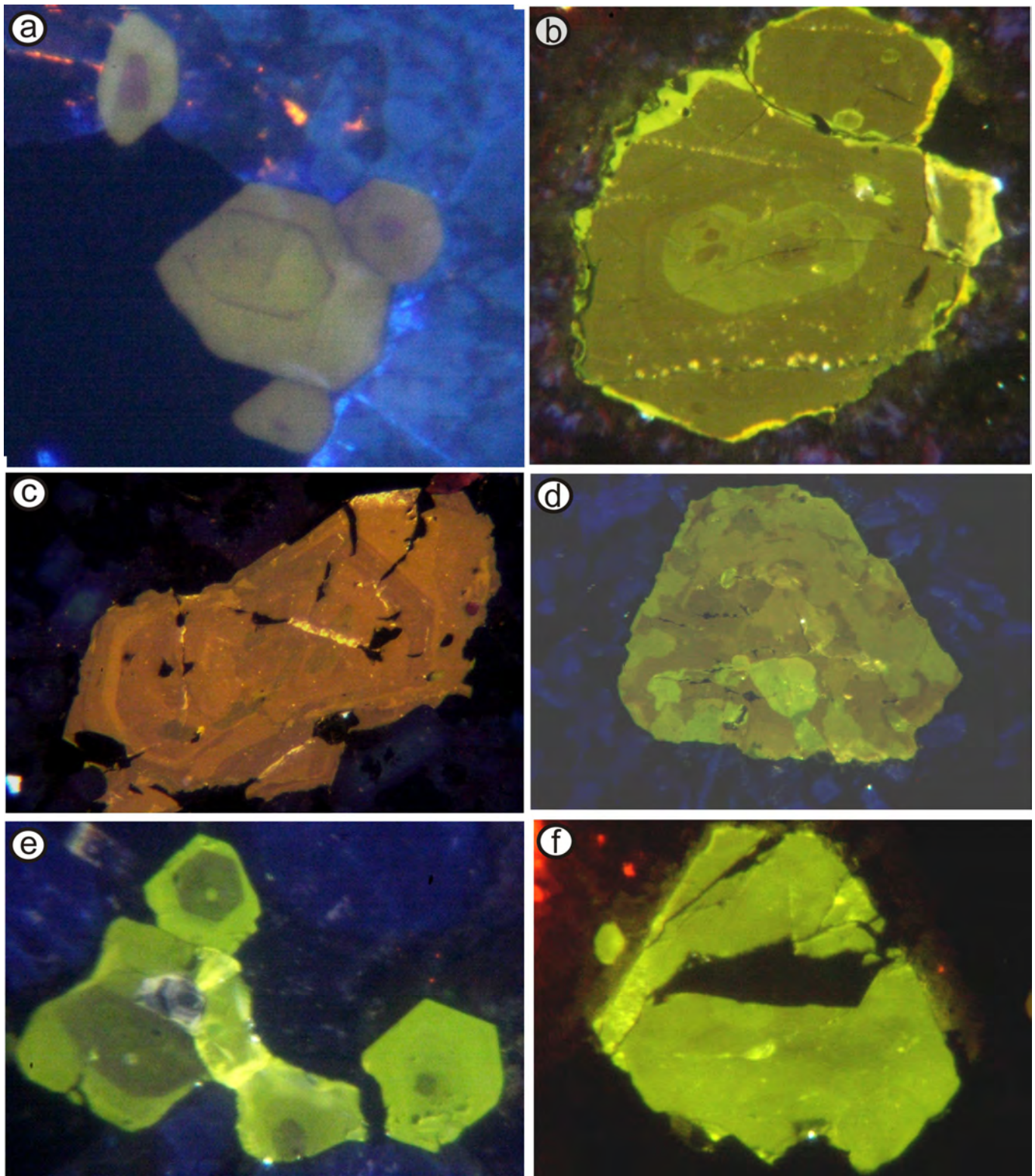
Figure 11: Representative apatite of fresh and altered host-rock from selected porphyry deposits in BC: (a) Apatite from least altered porphyritic monzonite of the Bootjack Stock, Mount Polley, showing zoned yellow-brown luminescence with a brownish phase occurring in the core and as narrow zone (PTB042). (b) Mount Polley apatite occurring with K-feldspar+magnetite alteration showing green-luminescent apatite has overgrown brown-luminescent apatite (PTB045). (c) Apatite from least-altered granodiorite host-rocks, Huckleberry, showing zoned brown to brick-red luminescence (HDM024). (d) Huckleberry apatite occurring with K-feldspar alteration and sulphide mineralization showing brown-luminescent apatite has been replaced by complex bodies of green-luminescent apatite (HDM022-2). (e) Apatite from least altered quartz monzonite host-rock, Endako porphyry Mo, showing zoned apatite with brown luminescence core and green rim (EDM003). (f) Endako apatite occurring with typical K-feldspar alteration showing dominantly green luminescence with remnant of brown-green luminescent apatite (EDM 026).

primary igneous magnetite by its occurrence in veins but disseminated hydrothermal magnetite may texturally be similar to magmatic magnetite. Igneous magnetite in host-rocks at Island Copper typically contain higher Ti contents of >1.5% TiO_2 relative to hydrothermal magnetite which contains <0.5% TiO_2 (Arancibia and Clark, 1996). Trace elements of magnetite such as Ti, V, Mn, Ca and Al can also be used to discriminate magnetite occurring in a range of deposit types (Dupuis and Beaudoin, 2011).

Magnetite is a common mineral in various porphyry deposits in British Columbia, occurring as an igneous accessory mineral in the host-rocks where it averages 1-5 volume percent, and as a hydrothermal mineral where it forms as veins and disseminations with K-silicate alteration. Sampling and petrographic analysis was mainly focused on commonly abundant pervasive magnetite rather than veinlet assemblage in order to compare magnetite in fresh and variously altered host-rocks. K-silicate alteration assemblages with magnetite are commonly overprinted by sericite or chlorite alteration which obliterates both magmatic and hydrothermal magnetite making textural distinctions between the two difficult. For the purpose of this study, magnetite associated with fresh or least-altered host-rocks (i.e., igneous) was compared with magnetite that formed in hydrothermally-altered and mineralized host-rocks. The latter represents effects of both K-silicate and overprinting sericite or chlorite alteration fluids.

Magnetite at Highland Valley: Igneous magnetite of the fresh Bethsaida granodiorite typically occurs as grains >100 μm in diameter and displays uniform pinkish color under reflected light (Figure 12a). The pink coloration is probably due to Ti content of magnetite. Therefore, these are probably titanomagnetite (Fe_3O_4-Fe_2TiO_4 solid solution) suggesting an igneous origin. More importantly small bodies of hematite occur mainly at the magnetite rim (Figure 12b).

Magnetite occurring with the K-silicate-altered Bethsaida granodiorite host-rocks and overprinted by green mica alteration locally have remnants of the pink magnetite in the core but the grains are largely replaced by hematite. Small grains of rutile are common near altered magnetite grains (Figure 12b).

Magnetite also occurs within altered remnants of mafic minerals which are mostly altered to chlorite (Figure 12c). Such magnetite usually displays a grey color under reflected light, and is surrounded by grains or needles of rutile. Titanite in these rocks is altered to mixtures of titanite, rutile and hematite (Figure 12b). Rutile is a common mineral occurring with chlorite, probably from the alteration of biotite, forming grains with chlorite and also as halos near chlorite (Figures 12e and 12f). The array of rutile grains near chlorite rims suggest that the Ti released during the alteration of biotite did not move far and that it formed rutile within the parent mineral.

Magnetite at Mt. Polley: Magnetite occurs in intrusive rocks at Mt. Polley ranging from 1 to 4 volume percent. Magnetite occurring with the least-altered host plagioclase porphyry rocks appears as coarse grains (>100 μm) with uniform pink color (titanomagnetite?) with no internal structures when examined under reflected light microscope (Figure 13a). The magnetite commonly has a rim of titanite as an overgrowth with some titanite crystals grow perpendicular on the magnetite surface. Hematite rims were not observed in the studied samples. Altered-mineralized samples from the same plagioclase porphyry were not available. Magnetite occurring with a high-grade mineralized diorite shows distinctly different texture. Altered magnetite grains have a pink magnetite core surrounded by hematite, similar to those at Highland Valley. Remnants of magnetite are less pinkish, and hematite clearly replaces magnetite (Figure 13b). Small grains or lamella of rutile occur inside or near magnetite grain.

Magnetite at Huckleberry: Magnetite from the Huckleberry porphyry deposit is similar to those from Mt. Polley. Magnetite occurring with fresh granodiorite displays a uniform pink color under reflected light microscope (Figure 14a). Titanite, locally altered to rutile, occurs at the rim. Magnetite grains occurring with mineralized granodiorite with K-feldspar and overprinting sericite-chlorite alteration (Figure 14c) show remnants of pink magnetite in their cores with rims replaced by hematite. In most cases, most or the entire magnetite grains are replaced by hematite.
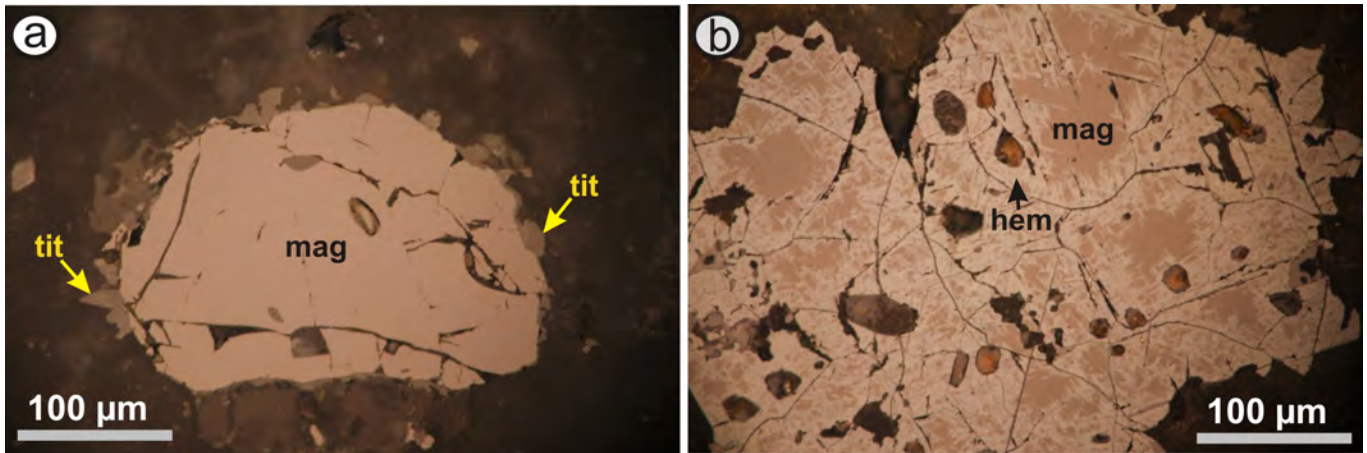
Magnetite at Endako: Magnetite occurring with fresh quartz monzonite (Figure 15a) shows uniform pink color and rim of grey hematite (Figure 15b). Magnetite grains occurring with K-feldspar and sericite altered and mineralized quartz monzonite show remnants of pink magnetite in the cores that are replaced by hematite around the rims (Figure 15c). Hematite has uniform textures near the core but towards the rim, the magnetite texture becomes spongy with quartz and other hydrothermal minerals filling the pore spaces. This probably represents a
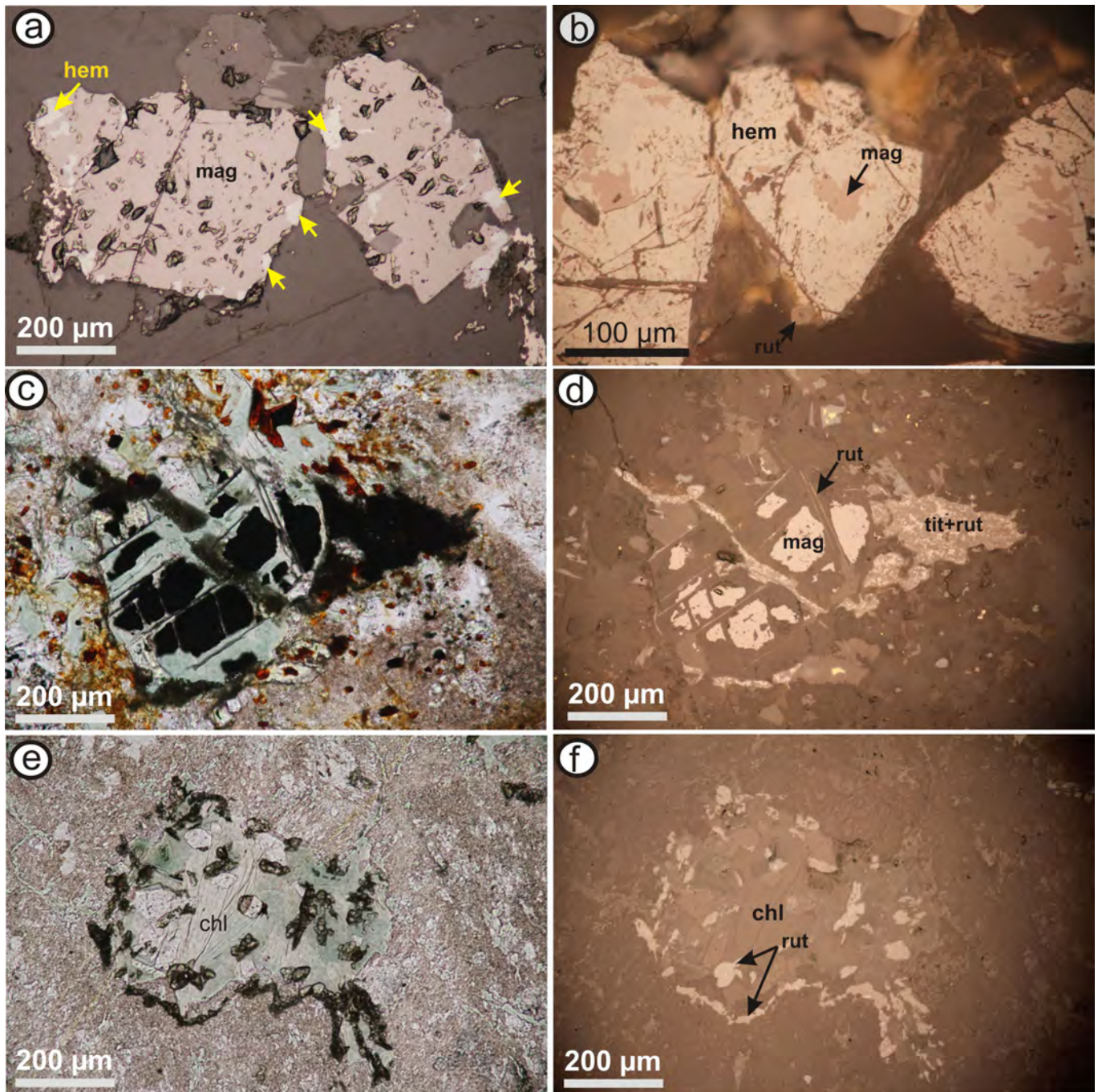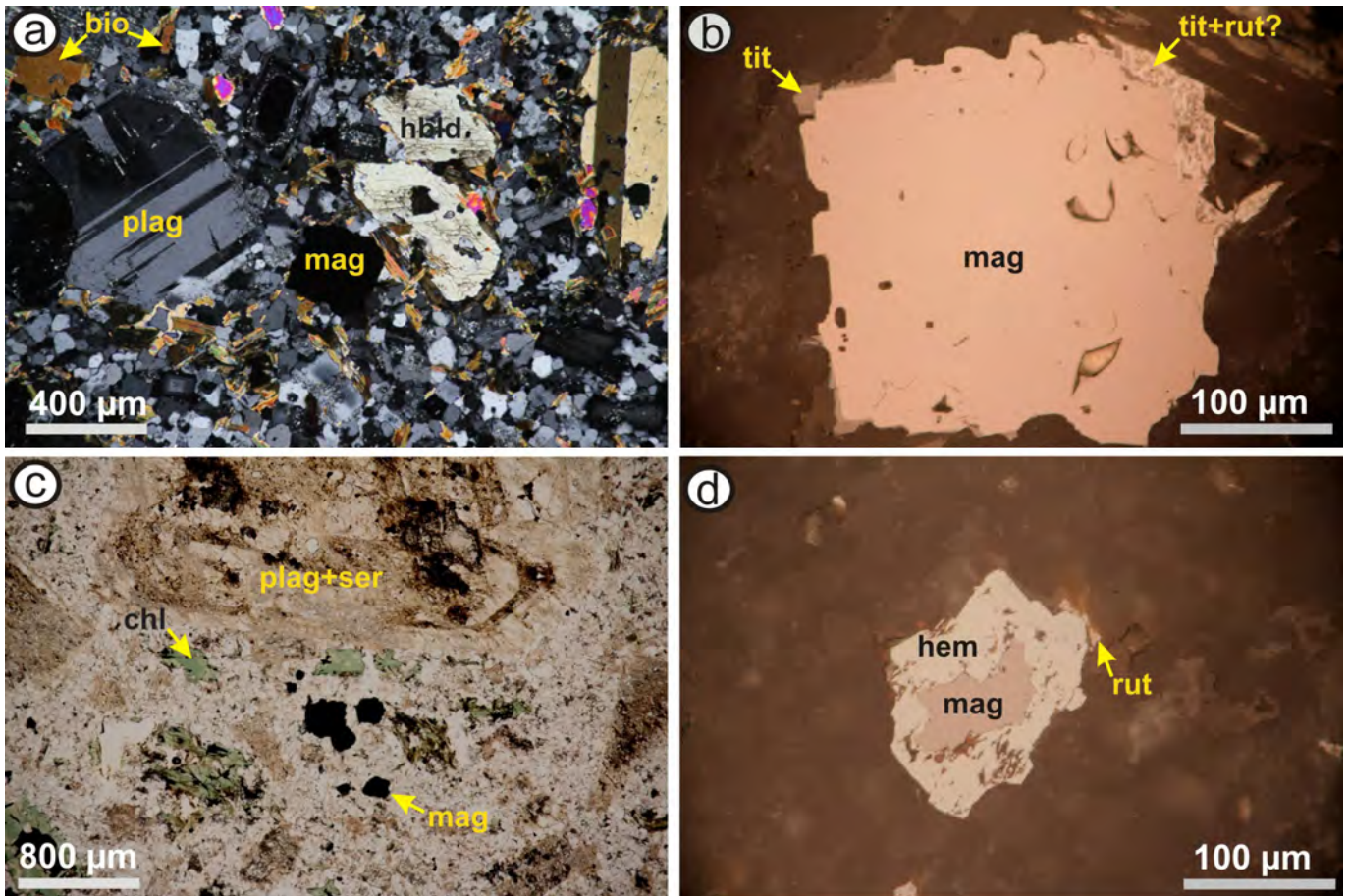
Figure 12: Magnetite-hematite occurring with fresh and altered rocks at Highland Valley: (a) Magnetite occurring with fresh Bethsaida granodiorite displaying uniform pink color under reflected light. Small bodies of hematite occur mainly at the magnetite rim (ALW-5). (b) Magnetite occurring with K-silicate altered Bethsaida granodiorite overprinted by green mica alteration from Valley pit showing much of the pink magnetite (core) is replaced by hematite; reflected light (HLV-3). (c) Magnetite bodies associated with chlorite (probably after hornblende?) from Bethlehem granodiorite (Huestis pit) overprinted by green muscovite and epidote alterations showing magnetite with grey color surrounded by rutile and altered titanite (mixture of titanite and rutile); reflected light (BET-2). (e and f) Plan polarized (e) and reflected light (f) images of a chlorite body (after biotite?) occurring with grains of rutile. Note that rutile crystals occur with chlorite and also form a halo near chlorite; Bethlehem granodiorite (Huestis pit) overprinted by green muscovite and epidote alterations (BET-3). [mag = magnetite, hem = hematite, rut = rutile, tit = titanite, chl = chlorite, hbld = hornblende, plag = plagioclase, bio = biotite, ser = sericite]. Reflected light images are obtained using air lenses.
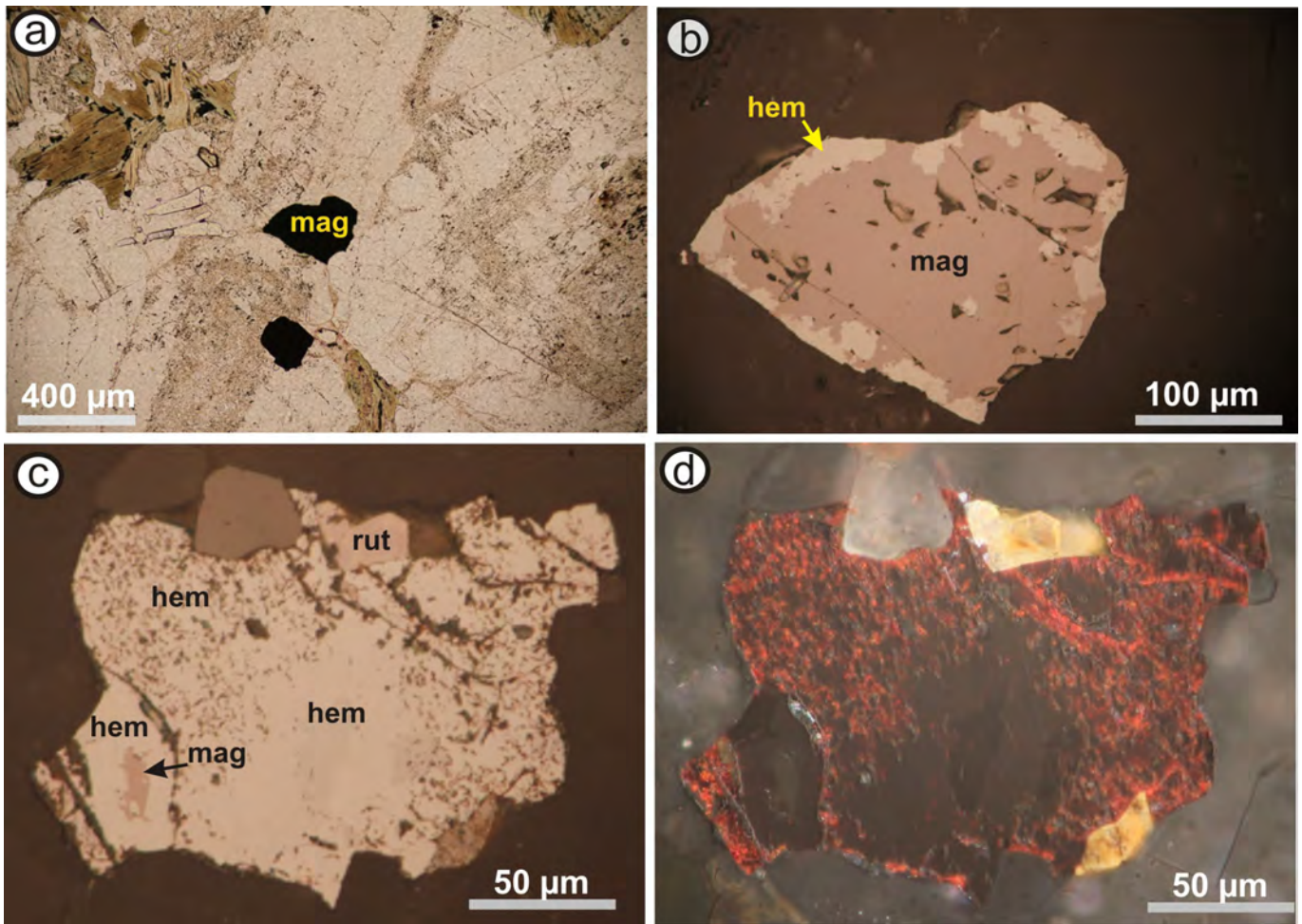
Figure 13: Magnetite-hematite occurring with fresh and altered rock at Mt. Polley: (a) Magnetite occurring with fresh to weakly K-silicate (K-feldspar) altered plagioclase porphyry showing uniform pink color surrounded by a rim of titanite. Note perpendicular growth of titanite crystal on the magnetite surface; reflected light (PTB045). (b) Magnetite occurring with high copper grade in diorite showing remnant of pink magnetite which is replaced by grey hematite (PTB047).

Figure 14: Magnetite-hematite occurring with fresh and altered rock at Huckleberry deposit: (a) Cross polarized image of fresh granodiorite with magnetite (HDM024). (b) Magnetite of figure (a) showing uniform pink color and titanite occurring at the rim. (c) Plane polarized light of altered granodiorite with K-feldspar and overprinting sericite-chlorite alteration and disseminated magnetite (HDM022-2). (d) Magnetite grain from figure (c) showing pink magnetite at core is replaced by hematite.

20

Figure 15: Magnetite-hematite occurring with fresh and altered rock at Endako: (a) Magnetite from unaltered quartz monzonite surrounded by K-feldspar and biotite; plan polarized light (EDM003). Magnetite grain from figure (a) showing uniform pink color and rim of grey hematite; air reflected light. (c) Magnetite occurring with altered (K-feldspar and sericite) quartz monzonite with only remnant of pink magnetite remained in the core. Most of the magnetite is replaced by hematite. Hematite has uniform texture in the center and is surrounded by spongy textured magnetite at the rim; reflected light (EDM026). (d) Same magnetite grain as in (c) but using cross polarized light showing characteristic red internal reflection of spongy hematite along grain boundaries and yellow internal reflection of rutile. The darker core of uniform hematite is due to anisotropy of hematite. Weak bireflectance of the uniform hematite is visible in figure (c).

more advanced stage of magnetite replacement. Overall, the magnetite at Endako is similar to that at Highland Valley, but the hematite rims are more abundant at Endako.

It can be concluded from these observations that magnetite in fresh or weakly altered host-rocks regardless of the type of host-rocks, displays uniform pink color under the reflected light microscope which is similar to the igneous titanomagnetite commonly occurring in granitoid rocks. Magnetite, moreover, in all fresh or weakly altered host-rocks has a rim of hematite or titanite. It is possible that hematite and titanite were formed as secondary phase during low levels of alteration (e.g., Piccoli et al., 2000). However, the scattered body texture of hematite and crystalline shape of titanite is indicative of these phases having formed during late stage of igneous crystallization

during which higher oxidizing conditions prevailed. Continuation of this process with decreasing temperature during subsequent hydrothermal stage can result in sulphide mineralization (Einaudi et al., 2003). Therefore, hematite and titanite rims on magnetite, similar to brown apatite zoning, may provide clues to the oxidation state and fertility of the host-rocks.

Magnetite grains occurring with altered host-rocks display remnant of pink magnetite replaced by hematite. This implies that during the hydrothermal event, from K-silicate alteration to overprinting sericite or chlorite alteration, the oxidation of the porphyry systems progressively increased and hematite become the stable phase. The Ti released or liberated from titanomagnetite commonly forms rutile lamella or grains within or near magnetite-hematite bodies.

Hematite becomes the dominant Fe-oxide phase during the advanced stages of alteration forming spongy hematite after magnetite that is cemented by hydrothermal quartz.

Summary of key textural characteristics of apatite and magnetite:

From the above field and petrographic observations, specific textural evidences can be used to characterize the following indicator minerals associated with porphyry deposits:

1. Apatite occurring with unmineralized igneous host-rocks is typically euhedral and displays yellow and brown luminescence.
2. Apatite occurring with unmineralized host-rocks displays uniform to concentric zoned texture under CL. The zoned apatite commonly has a core and/or zones of brown luminescent phase.
3. Apatite occurring with K-silicate altered host-rock in all studied deposits displays green color luminescence. The green luminescence replaces yellow or yellow-brown luminescent apatite and less commonly occurs as thin overgrowth zone on apatite.
4. Apatite occurring with muscovite alteration displays grey luminescence. The grey luminescence replaces green luminescence.
5. Magnetite in fresh or weakly altered host-rocks in all deposits, regardless of the type of host-rocks, displays uniform pink color when examined under the reflected light microscope. The pink magnetite is similar to the igneous titanomagnetite commonly occurring in granitoid rocks.
6. Magnetite in all fresh or weakly altered host-rocks has a rim of hematite or titanite. The hematite rim appears to be more typical in calc-alkalic host-rocks and the titanite rim in alkalic host-rocks.
7. Magnetite grains occurring with altered host-rocks in all studied porphyry deposits display remnant of pink magnetite commonly in the core replaced by hematite at the rim.
8. Advanced stages of magnetite alteration by hydrothermal fluids forms spongy hematite that is cemented by hydrothermal quartz.

CHEMICAL CHARACTERISTICS

Apatite (general formula $Ca_5[(PO_4)_3(OH,F,Cl)])$ may concentrate a high proportion of REE, Sr, Mn, Na, U

and Th, and other trace elements in its structure making it potentially a sensitive recorder of the trace-element chemistry of the rock system. This is due to various common lattice substitutions in apatite structure (see above). The incorporation of trace elements in accessory apatite depends on the geological environment of host-rock formation such as the SiO_2 activity, fO_2, total alkalis, the aluminum saturation index (ASI) and subsequent alteration processes (e.g., Sha and Chappell, 1999; Belousova et al., 2002). These parameters, particularly the relationship between fractionation and oxidation state, are critical to the development of magma-related porphyry and hydrothermal ore systems (Blevin and Chappell, 1995). Thus, the geochemical signatures recognized in apatite from specific rock types and alteration assemblages potentially can provide discriminants that make apatite useful as an indicator mineral in mineral exploration.

As part of establishing criteria to discriminate porphyry related indicator minerals, selected grains of apatite were analyzed by electron microprobe. Textural characteristics and physical properties such as luminescence were recorded for each analysis in order to evaluate if a systematic changes in chemical composition exists for observed textural variations.

Results of the chemical analyses of apatite grains from both unaltered and altered host-rocks by electron microprobe are given in Appendix 2. Detection limits are reported in Appendix 2 and shown in the graphs. Some analyses are shown as below detection limit (< D.L.) because they are associated with high error. The absolute values of these analyses are not acceptable but are shown graphically to see if there is a relationship between apatite type and element concentration above or below detection limit. Results emphasizing distinct compositional trends are shown graphically in Figures 16 to 20. These diagrams are also coded according to the nature of the hostrock and are coloured according to the apatite luminescence. In general, there were four luminescence colors in the studied apatite samples: yellow, brown, green and grey with the grey occurring only at Highland Valley samples. As discussed above, yellow and brown color luminescence commonly represent unaltered apatite and green and grey luminescence represent apatite associated with K-silicate and phyllic alterations, respectively.
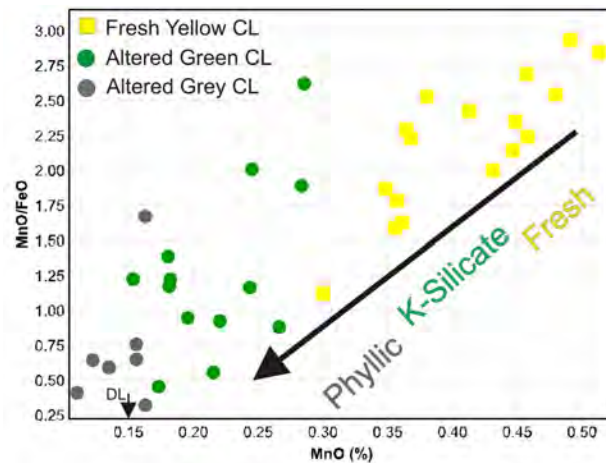
Apatite composition at Highland Valley

Comparison of chemical composition of fresh and alteration related apatite at Highland Valley shows that nearly all fresh apatite have Na_2O contents of 0.1 to 0.2%
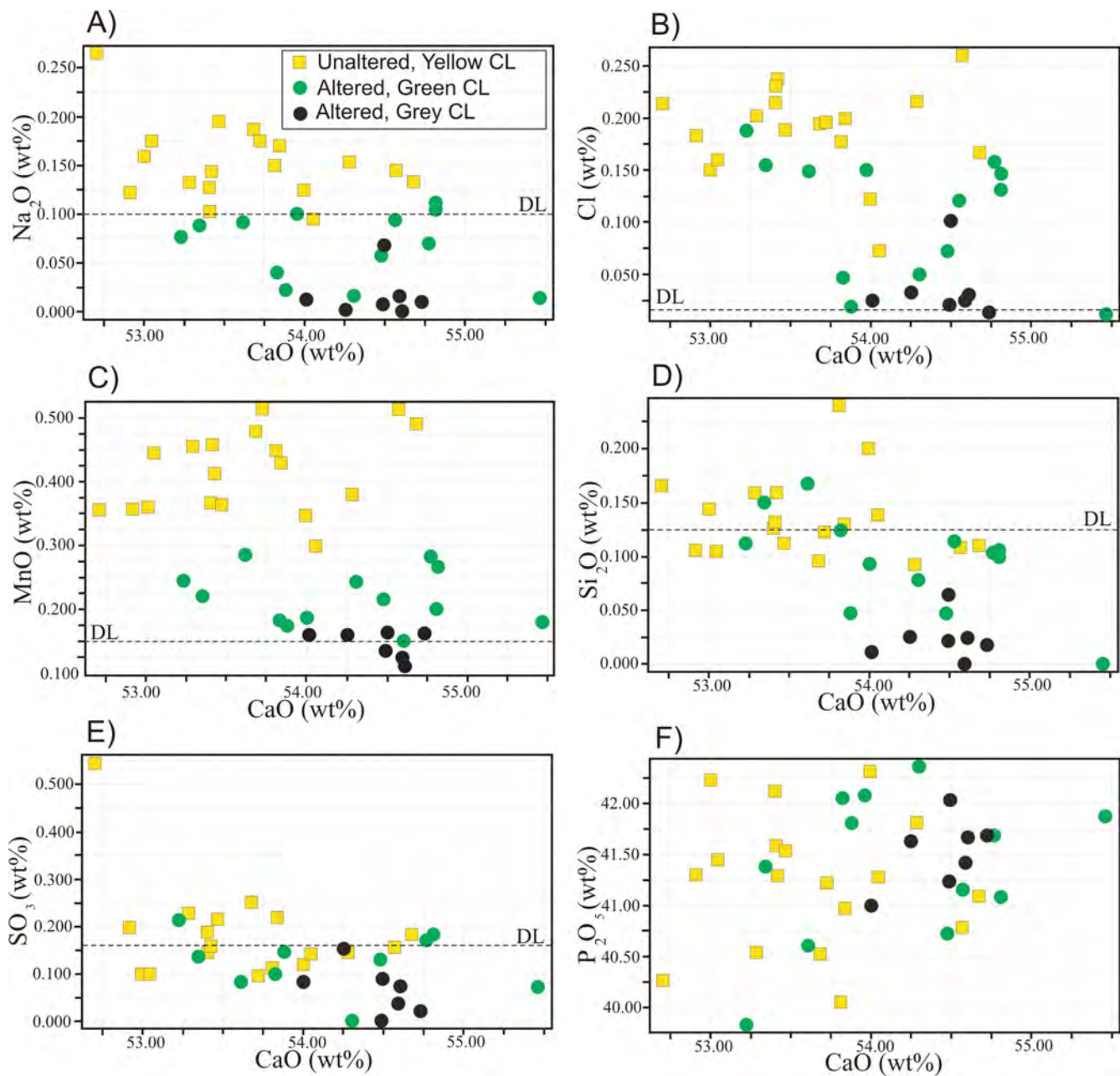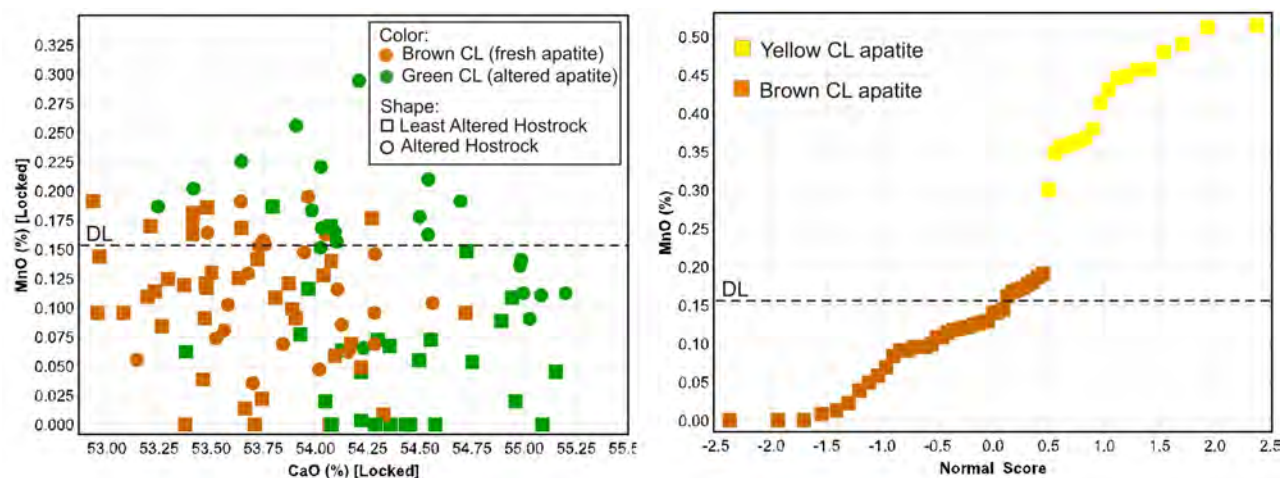
Figure 16: Chemical composition of apatite in fresh and altered host-rocks, Highland Valley (DL = detection limit).

Figure 17: Binary diagram showing correlation of the luminescence with the MnO/FeO ratio, Highland Valley.

Figure 18: (a) Comparison of MnO concentrations in fresh and altered apatite in samples from Mt. Polley, Huckleberry and Endako. (b) Probability plot of MnO concentration in fresh yellow-luminescent apatite and fresh brown-luminescent apatite showing that the latter has significantly less Mn.

while altered apatite has near or below detection limit Na_2O (Figure 16a). Most of the analyses for sulphur were below detection limit but samples with concentrations above the detection limit were mainly from fresh rocks with yellow-luminescent apatite (Figure 16e). Similar relationships can be seen for SiO_2 contents. Therefore, altered apatites have lower concentrations of Na and S relative to fresh apatite indicating that these element were depleted from apatite during subsequent hydrothermal alteration.

Analyses of Mn gives better results with most concentrations above the detection limit. MnO has the highest concentrations in fresh yellow-luminescent apatite (0.3-0.5% MnO) with the altered green-luminescent apatite typically containing less than 0.3% MnO (Figure 16c). The grey-luminescent apatite has the lowest MnO concentration near or below the detection limit of 0.15% MnO. Similar trends can be seen for Cl (Figure 16b). The decrease in MnO concentration is correlated with the decrease in MnO/FeO ratio (Figure 17). Therefore, during alteration of yellow-luminescent, Mn-rich apatite, Mn is progressively depleted from the apatite structure and overall Fe/Mn ratio increased causing the typical green-luminescent apatite related to K-silicate alteration. There is a significant loss of Mn during the intense muscovite alteration that results in the loss of luminescence, thus producing the grey-luminescent apatite (Figure 17).

It is notable that selected altered samples from Highland Valley were moderate to strongly-altered and therefore these samples did not contain remnants of unaltered apatite (e.g., yellow-luminescent apatite). Similarly, the unaltered host-rocks did not display visible alteration or secondary apatite because fresh samples were taken from sites that were several kilometres away from the main mineralization. Therefore, at Highland Valley there is a good correlation between host-rock, i.e., fresh vs. altered, and apatite luminescence, as indicated in the figures.
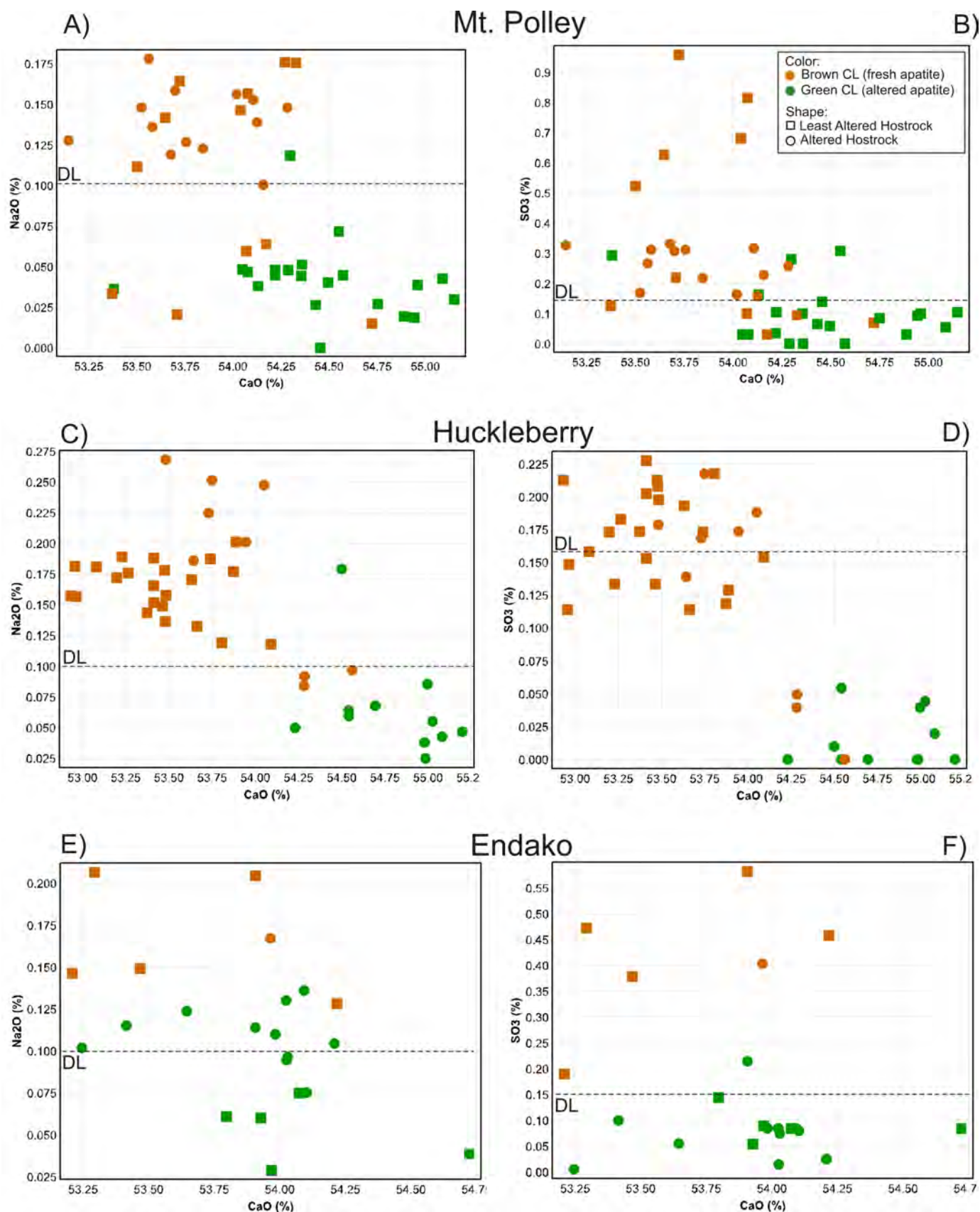
Apatite composition at other porphyry deposits

Selected apatite samples from Mt. Polley, Huckleberry and Endako porphyry deposits were analyzed. As discussed above, unaltered apatite in these deposits commonly occurs as brown-luminescent apatite and the K-silicate alteration related apatite displays green luminescence. The grey-luminescent apatite does not occur because phyllic alteration does not occur significantly in these deposits, or it was not sampled.
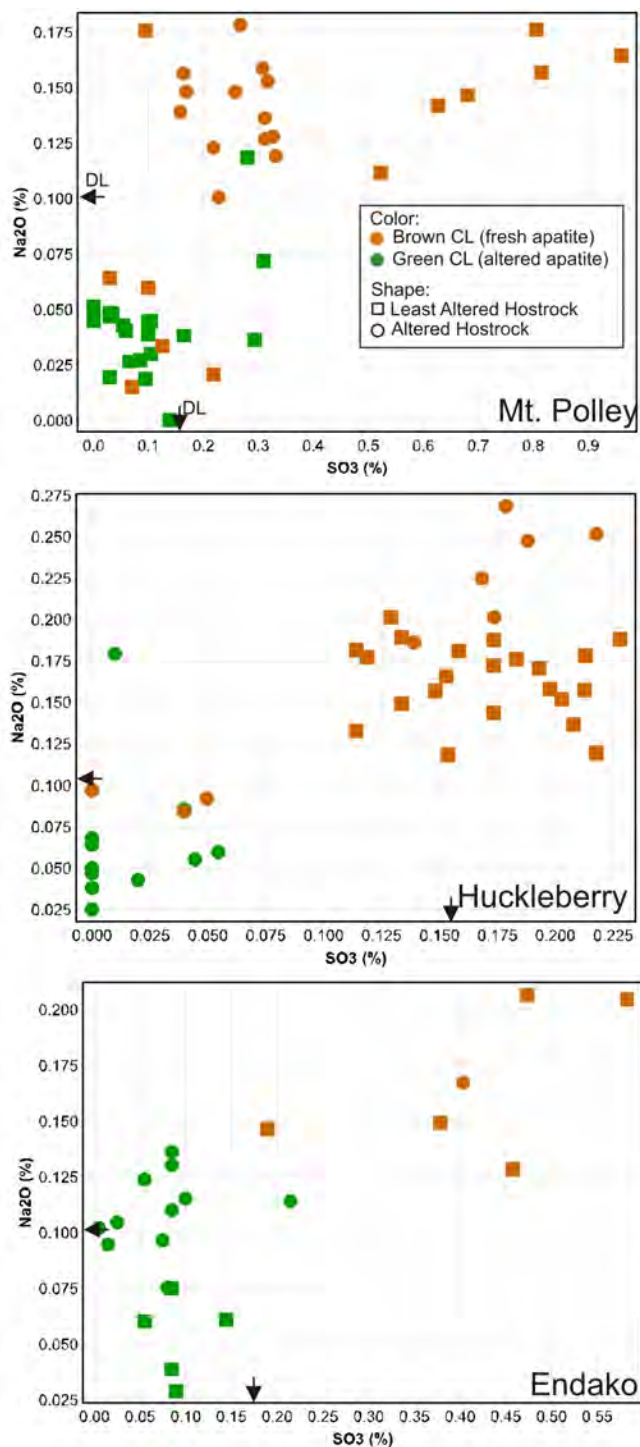
Unlike Highland Valley, samples from these deposits do not show meaningful correlation between apatite luminescence and MnO concentration (Figure 18a). This is largely because MnO concentration of apatite in these samples was significantly lower than those from Highland Valley apatites (Figure 18b). Thus, MnO concentrations of fresh apatite for Mt. Polley, Huckleberry and Endako were below detection limit for most of the analyzed samples. This explains the lack of yellow luminescence and the existence of brown luminescence in fresh apatite of these three deposits. Some other trace elements may have contributed to the brown color luminescence. On the basis on these limited samples it is not clear what controls the common occurrence of brown apatite as they are from a range of host-rocks and compositions.

Given the low concentration of Mn, it is possible to envisage that other elements contributed to the change from brown to green luminescence during the

Figure 19: Chemical composition of unaltered and altered apatite occurring with fresh and K-silicate altered host-rocks with no significant phyllic alteration overprint.

Figure 20: Binary diagram showing correlation between luminescence and Na$_2$O and SO$_3$ concentrations in fresh and altered apatite.

(Kempe and Götze 2002). Therefore, minor changes in Mn concentration and resulting change in the Mn/Fe ratio in the brown luminescent apatite may have contributed to the development of green-luminescent apatite but it was not detected due to overall low concentration of Mn and inadequate detection limit during this study for these samples.

Elements such as Cl and S commonly have higher concentrations in these deposits relative to that at Highland Valley. When comparing fresh and altered apatite, the green-luminescent apatite has lower concentrations of Na$_2$O and SO$_3$ (commonly below detection limit) than the fresh brown-luminescent apatite (Figure 19). Therefore, these elements were lost from apatite during K-silicate alteration, similar to Highland Valley (Figure 20). Moreover, most of the altered apatite samples show slightly higher concentrations of Ca (around 1%). Similar relationship were noted for apatite from Highland Valley (see Figure 16b and 16f). This probably results from the loss of trace elements during hydrothermal alteration and constraints of closure on analytical data totals to 100 wt.%. Therefore, Ca was probably not added but other trace elements were lost during alteration.

CONCLUSIONS AND RECOMMENDATIONS

This scoping study of accessory resistate minerals in porphyry Cu deposits indicates that some minerals can be effective recorders of the hydrothermal effects related to mineralization, and that they can record the variably effects of different types and intensities of alteration typical of the porphyry environment. This study further highlights the wide range of characteristics that apatite and Fe-oxide minerals can have, and emphasizes their potential use as indicators of porphyry Cu deposits. Some of the main conclusions of this study are:

1. Apatite is a ubiquitous accessory mineral which occurs in a wide range of host-rocks and commonly incorporates a wide range of trace elements and is capable of recording both magmatic and hydrothermal processes. It is also resistant to weathering, making it a robust, easy to collect recorder of mineralization-related alteration.
2. Apatite occurs as grains commonly 50 to 200 μm in fresh and altered host-rock making it possible to collect by conventional sieving and mineral separation methods.

K-silicate alteration. However, the control on change in luminescence is the Mn/Fe ratio and not the absolute concentration ratio of Mn or Fe. Kempe and Götze (2002) have shown that there is no direct correlation between CL intensity in apatite and absolute concentration of Mn or Fe. Similar relationships are shown for the effect of REE

3. Apatite in fresh host-rocks associated with porphyry deposits displays yellow, yellow-brown and brown luminescence. The yellow luminescence is caused by Mn (0.3 to 0.5% MnO). The Mn content of brown-luminescent apatite is low (<0.2 MnO) and other trace elements, such as REE, probably contributed to the brown luminescence.

4. Primary igneous apatites in plutonic rocks that host porphyry deposits commonly display concentric zoning. The zoned apatite commonly has a core and/or zones of brown luminescent phase. The composition of these zones reflects magmatic processes such as oxidation state, melt mixing and sulphur saturation. Therefore, apatite can be used to study fertility of the pluton for hosting porphyry deposits.

5. Apatite occurring with K-silicate altered host-rocks from all deposits displays green luminescence. The green luminescence replaces yellow or brown luminescent apatite and less commonly overgrows it. The green luminescence is caused by lower Mn/Fe ratio and not the absolute concentrations of Mn or Fe. Other trace elements such as Cl, Na and S are also depleted from apatite during the K-silicate alteration.

6. Apatite occurring with mineralization and intense muscovite alteration displays characteristic grey luminescence as a result of a significant loss of Mn during phyllic alteration. Such fluids were not developed in alkalic porphyry deposits; therefore the grey-luminescent apatite is not expected to widely occur in alkalic deposits.

7. There is a correlation between the intensity of alteration and the degree of development of green or grey luminescence in individual apatite grains. Therefore, such evidence as recorded in apatite can be used to estimate the intensity of mineralization in the parent host-rock.

8. Magnetite occurs as a common accessory mineral associated with the host-rock of porphyry deposits, where it displays a uniform pink color in reflected light, indicating high titanium contents (e.g. titanomagnetite) and a probable igneous origin.

9. Magnetite in fresh or weakly altered host-rocks have rims of hematite or titanite indicating an increase in the oxidation state of the latest crystallizing melt which ultimately led to the generation of the porphyry deposit. Therefore, such texture may be used to evaluate fertility of the pluton.

10. Magnetite grains occurring with altered host-rocks in all studied porphyry deposits have remnants of pink magnetite surrounded by hematite. This implies that during the main hydrothermal alteration events, the oxidation state of the hydrothermal part of the porphyry systems progressively increased and hematite become the stable phase. The Ti liberated from titanomagnetite commonly forms rutile lamella or grains within or near magnetite-hematite bodies.

11. Advanced stages of magnetite alteration forms spongy hematite cemented by hydrothermal quartz. Thus, the magnetite-hematite-titanite-rutile-quartz aggregate with various proportion of each mineral forms a more resistate grain which can be easily separated from sediments because of its magnetic property and high density.

Recommendations

These results provide a first step towards developing a better understanding and, ultimately, for the use of resistate minerals as indicators to better determine the presence and locations of porphyry copper exploration. Observations during this study suggest that several other resistate minerals could provide promising potential for use as indicator particularly titanite and rutile. However, there are several key questions that need to be addressed:

1. How abundant is occurrence of apatite in sedimentary rocks associated with erosion of porphyry deposits? and how large is the detectable footprint of apatite?

2. What is the optimal sampling density and sample size to detect the mineralization?

3. How different is apatite distribution in sediments in various erosional environment, e.g., glacial versus non glacial?

To answer these questions, study of overburden sediments in various geological environments is recommended.

Another important avenue that requires investigation is development of mineral separation and examination protocols. In particular:

1. What are the optimal sample size and mineral separation techniques for apatite?

2. What tools can be used to effectively and timely recognize indicator apatite grains?

To answer these questions, conventional heavy mineral separation techniques (e.g., McClenaghan, 2005) need to be tested. More importantly, application of advanced mineral

screening techniques, such as MLA (Mineral Liberation Analysis), need to be tested. For apatite, particularly, use of SEM-CL and development of corresponding image analysis is critical.

Similar questions need to be answered for Fe-oxide and other PIMs.

A parallel study is required to further characterize apatite, magnetite and other resistate minerals in porphyry copper deposits.

ACKNOWLEDGEMENTS

REFERENCES

Alva Jimenez, T.R, 2011, Variation in hydrothermal muscovite and chlorite composition in the Highland Valley porphyry Cu-Mo District, British Columbia, Canada: M.Sc. Thesis, University of British Columbia, 234 p.

Arancibia, O.N., and Clark, A.H., 1996, Early magnetite-amphibole-plagioclase alteration-mineralization in the Island copper porphyry copper-gold-molybdenum deposit, British Columbia: Economic Geology, v. 91, p. 402-438.

Averill, S.A., 2001, The application of heavy indicator mineralogy in mineral exploration, with emphasis on base metal indicators in glaciated metamorphic and plutonic terrain: in McClenaghan, M.B., Bobrowsky, P.T., Hall, G.E.M., and Cook, S.J., eds., Drift Exploration in Glaciated Terrain, Geological Society of London Special Publication 185, p. 69-82.

Averill, S.A., 2007, Recent advances in base metal indicator mineralogy: An update from Overburden Drilling Management Limited: Explore, v. 134, p. 2-6.

Ballard, J.R., Palin, J.M. and Campbell, I.H., 2002, Relative oxidation states of magmas inferred from Ce(IV)/Ce(III) in zircon: application to porphyry copper deposits of northern Chile: Contributions to Mineralogy and Petrology, v. 144, p. 347–364.

Barnett, C. and Williams, P.M., 2009, Using geochemistry and neural networks to map geology under glacial cover: Geoscience BC, Report 2009-3, 26p.

Bath, A.B. and Cooke, D., 2008, The importance of biotite for the deposition of sulfides at the Lorraine Cu-Au porphyry deposit, north-central British Columbia, in Shallow and Deep-Level Alkalic Deposits, Porphyry Module, K. Simpson and T. Bissig (eds.), unpublished report, Mineral Deposit Research Unit, University of British Columbia and Centre of Excellence in Ore Deposit Research, University of Tasmania, p. 7.1-7.30.

Bath, A.B., Logan, J.M. and Kamenetsky, V.S., 2006, Apatite in Cu-sulfide ore from the Mount Polley alkalic porphyry, BC Canada (abstract); 16th Annual V.M Goldschmidt Conference, Geochimica et Cosmochimica Acta, v. 70, no. 18, suppl. 1, p. A40.

Belousova, E.A., Griffin, W.L., O'Reilly, S.Y. and Fisher, N.I., 2002, Apatite as an indicator mineral for mineral exploration: trace-element compositions and their relationship to host rock type; Journal of Geochemical Exploration, v. 76, p. 45–69.

Bishop, S.T., Heah, T.S., Stanley, C.R. and Lang, J.R., 1995, Alkalic intrusion hosted copper gold mineralization at the Lorraine deposit, north-central British Columbia: in Porphyry Deposits of the Northwestern Cordillera of North America, T.G. Schroeter (ed.), Canadian Institute of Mining and Metallurgy, Special Volume 46, p. 623–629.

Blevin, P.L., Chappell, B.W., 1995, Chemistry, origin and evolution of mineralised granites in the Lachlan Fold Belt, Australia: the metallogeny of I- and S-type granites: Economic Geology, v. 90, 1604–1619.

Bouzari, F., and Clark, A.H., 2006, Prograde Evolution and Geothermal Affinities of a Major Porphyry Copper Deposit: The Cerro Colorado Hypogene Protore, I Región, Northern Chile: Economic Geology, v. 101; p. 95-134.

Bysouth, G.D., and Wong, G.Y.,1995, The Endako molybdenum mine, central British Columbia: an update: in Porphyry Deposits of the Northwestern Cordillera of North America, T.G. Schroeter (ed.), Canadian Institute of Mining and Metallurgy, Special Volume 46, p. 697-703.

Carson, D.J.T. and Jambor, J.L., 1974, Mineralogy, zonal relationships and economic significance of hydrothermal alteration at porphyry copper deposits, Babine Lake Area, British Columbia: Canadian Institute of Mining and Metallurgy, Bulletin, v. 67, p. 110–133.

Casselman, M.J., McMillan, W.J. and Newman, K.M., 1995, Highland Valley porphyry copper deposits near Kamloops, British Columbia: a review and update with emphasis on the Valley deposit: in Porphyry Deposits of the Northwestern Cordillera of North America, T.G. Schroeter (ed.), Canadian Institute of Mining and Metallurgy, Special Volume 46, p. 161–191.

Clark, A.H., 1993, Are outsize porphyry copper deposits either anatomically or environmentally distinctive?, in Whiting, B.H., Hodgson, C.J., and Mason, R., eds., Giant ore deposits: Society of Economic Geologists Special Publication 2, p. 213-283.

Cox, D.P., 1985, Geology of the Tanama and Helecho porphyry copper deposits and vicinity, Puerto Rico: U .S. Geological

Survey Professional Paper 1327, 59 p.

Czamanske, G.K., Force, E.R. and Moore, W.J., 1981, Some geologic and potential resource aspects of rutile in porphyry copper deposits: Economic Geology, v. 76, p. 2240–2256.

Desborough, G.A. and Sharp, W.N., 1978, Tantalum, uranium, and scandium in heavy accessory oxides, Climax molybdenum mine, Climax, Colorado: Economic Geology, v. 73, p. 1749–1751.

Deyell, C.L. and Tosdal, R.M., 2005, Alkalic Cu-Au deposits of British Columbia: sulfur isotope zonation as a guide to mineral exploration: in Geological Fieldwork 2004, BC Ministry of Energy, Mines and Petroleum Resources, Paper 2005-1, p. 191–208.

Dupuis, C., and Beaudoin, G., 2011, Discriminant diagrams for iron oxide trace element fingerprinting of mineral deposit types: Mineralium Deposita, v. 46, p. 319–335.

Einaudi, M.T., Hedenquist, J.W., and Inan, E., 2003, Sulfidation state of hydrothermal fluids: The porphyry-epithermal transition and beyond: Society of Economic Geologists and Geochemical Society Special Publication 10, p. 285–313.Ethier, V.G., and Campbell, F.A., 1977, Tourmaline concentration in Proterozoic sediments of the southern Cordillera of Canada and their economics significance: Canadian Journal of Earth Sciences, v. 4, p. 2345-2383.

Farr, A., Meyer, S. and Bates, M., 2008, Airborne gravity survey, Quesnellia Region, British Columbia, Sander Geophysics Limited: Geoscience BC, Report 2008-8, 121 p.

Force, E.R., Djaswadi, S. and Van Leeuwen, T., 1984, Exploration for porphyry metal deposits based on rutile distribution: a test in Sumatra: United States Geological Survey, Bulletin, 1558-A.

Fraser, T.M., Stanley, C.R., Nikic, Z.T., Pesalj, R. and Gorc, D., 1995, The Mount Polley copper-gold alkalic porphyry deposit, south-central British Columbia: in Porphyry Deposits of the Northern Cordillera, T.G. Schroeter (ed.), Canadian Institute of Mining and Metallurgy, Special Volume 46, p. 609–622.

Griffin, W.L. and Ryan, C.G., 1995, Trace elements in indicator minerals: area selection and target evaluation in diamond exploration: Journal of Geochemical Exploration, v. 53, p. 311–337.

Gustafson, L.B. and Hunt, J.P., 1975, The porphyry copper deposit at El Salvador, Chile; Economic Geology, v. 70, p. 875–912.

Harris, D.C., 1989, The mineralogy and geochemistry of the Hemlo gold deposit, Ontario: Geological Survey of Canada, Economic Geology Report 38, 88 p.

Hedenquist, J.W., Arribas, A., Jr., and Reynolds, T.J., 1998, Evolution of an intrusion-centered hydrothermal system: Far Southeast-Lepanto porphyry and epithermal Cu-Au deposits, Philippines: Economic Geology, v. 93, p. 373-404.

Holland, H.D., 1972, Granites, solutions, and base metal deposits: Economic Geology, v. 67, p. 281-301.

Hoskin, P.W.O., 2005, Trace-element composition of hydrothermal zircon and the alteration of Hadean zircon from the Jack Hills, Australia: Geochimica et Cosmochimica Acta, v. 69, p. 637–648.

Ishihara, S., 1981, The granitoid series and mineralization: Economic Geology, 75th anniversary volume, p. 458–484.

Jackaman, W., Balfour, J.S. and Reichheld, S.A., 2009, QUEST-West Project geochemistry: field survey and data reanalysis, central British Columbia (parts of NTS 093E, F, J, K, L, M, N): in Geoscience BC Summary of Activities 2008, Geoscience BC, Report 2009-1, p. 7–14.

Jackson, A., and Illerbrun, K.,1995, Huckleberry porphyry copper deposit, Tahtsa Lake district, west-central British Columbia: in Porphyry Deposits of the Northwestern Cordillera of North America, T.G. Schroeter (ed.), Canadian Institute of Mining and Metallurgy, Special Volume 46, p. 313-321

Jago, C.J. and Tosdal, R.M., 2009, Distribution of alteration in an alkalic porphyry copper-gold deposit at Mount Milligan, central British Columbia (NTS 094N/01): in Geoscience BC Summary of Activities 2008, Geoscience BC, Report 2009-1, p. 33–48.

John, D.A., 1989, Evolution of hydrothermal fluids in the Park Premier stock, central Wasatch Mountains, Utah: Economic Geology, v. 84, p. 879-902.

Kempe, U. and Götze, J., 2002, Cathodoluminescence (CL) behaviour and crystal chemistry of apatite from rare-metal deposits: Mineralogical Magazine, v. 66, p. 151–172.

Kimura, E.T., Bysouth, G.D., Drummond, A.D., 1976, Endako: Canadian Institute of Mining, Metallurgy, and Petroleum, Special Volume 15, p. 444-454

Kowalczyk, P.K., 2009, QUEST-West geophysics in central British Columbia (NTS 093E, F, G, K, L, M, N, 103I): new regional gravity and helicopter time-domain electromagnetic data; in Geoscience BC Summary of Activities 2008, Geoscience BC, Report 2009-1, p. 1–6.

Lang, J.R., Lueck, B., Mortensen, J.K., Russell, J.K., Stanley, C.R. and Thompson, J.F.H., 1995, Triassic–Jurassic silica-undersaturated and silica-saturated alkalic intrusions in the Cordillera of British Columbia: implications for arc magmatism: Geology, v. 23, p. 451–454.

Liaghat, S. and Tosdal, R., 2008, Apatite chemical composition and textures as a probe into magmatic conditions at Galore Creek porphyry copper-gold deposit, British Columbia (abstract): 18th Annual V.M. Goldschmidt Conference, Geochimica et Cosmochimica Acta, v. 72, no. 12, p. A550.

Logan, J. M. and Mihalynuk, M.G., 2005, Regional geology and setting of the Cariboo, Bell, Springer and Northeast porphyry Cu-Au zones at Mount Polley, south-central British Columbia: in Geological Fieldwork 2004, BC Ministry of Energy, Mines and Petroleum Resources, Paper 2005-1, p. 249–270.

Mariano, A.N., 1988, Some further geological applications of cathodoluminescence: in Cathodoluminescence of Geological Materials, D.J. Marshall (ed.), Unwin Hyman, Boston, p. 94–123.

McClenaghan, M.B., 2005, Indicator mineral methods in mineral exploration: Geochemistry: Exploration, Environment, Analysis, v. 5, p. 233–245

McClenaghan, M. B. and Kjarsgaard, B. A., 2007. Indicator mineral and surficial geochemical exploration methods for kimberlite in glaciated terrain; examples from Canada; in Mineral Deposits of Canada: A synthesis of Major Deposit-Types, District Metallogeny, the Evolution of Geological Provinces, and Exploration Methods, (ed.) W. D. Goodfellow; Geological Association of Canada, Special Publication No. 4, p. 983-1006.

McMillan, W.J., Thompson, J.F.H., Hart, C.J.R. and Johnston, S.T., 1995, Regional geological and tectonic setting of porphyry deposits in British Columbia and Yukon Territory: in Porphyry Deposits of the Northwestern Cordillera of North America, T.G. Schroeter (ed.), Canadian Institute of Mining and Metallurgy, Special Volume 46, p. 40–57.

Moore, W.J., and Czamanske, G.K., 1973, Composition of biotites from unaltered and altered monzonitic rocks in the Bingham mining district, Utah: Economic Geology, v. 68, p. 269-274.

Mortensen, J.K., Ghosh, D.K. and Ferri, F.,(1995, U-Pb geochronology of intrusive rocks associated with copper-gold porphyry deposits in the Canadian Cordillera: in Porphyry Deposits of the Northwestern Cordillera of North America, T.G. Schroeter (ed.), Canadian Institute of Mining and Metallurgy, Special Volume 46, p. 142–158.

Nakada, S., 1991, Magmatic processes in titanite-bearing dacites, central Andes of Chile and Bolivia: American Mineralogist, v. 91, p. 548–560.

Nelson, J. L. and Bellefontaine, K.A., 1996, The geology and mineral deposits of north-central Quesnellia: Tezzeron Lake to Discovery Creek, central British Columbia: BC Ministry of Energy, Mines and Petroleum Resources, Bulletin 99, 112 p.

Nixon, G.T. and Peatfield, G.R., 2003, Geological setting of the Lorraine Cu-Au porphyry deposit, Duckling Creek Syenite Complex, North-central British Columbia: in BC Ministry of Energy, Mines and Petroleum Resources, Open File 2003-4, 24 p.

Panteleyev, A., Bailey, D.G., Bloodgood, M.A. and Hancock, K.D., 1996, Geology and mineral deposits of the Quesnel River–Horsefly map area, central Quesnel Trough, British Columbia (NTS 93A/5, 6, 7, 11, 13; 93B/9, 16,: 93G/1; 93H/4): BC Ministry of Energy, Mines and Petroleum Resources, Bulletin 97, 156 p.

Pettke, T., Audétat, A., Schaltegger, U. and Heinrich, C.A., 2005, Magmatic-to-hydrothermal crystallization in the W–Sn mineralized Mole Granite (NSW, Australia): Part II: Evolving zircon and thorite trace element chemistry: Chemical Geology, v. 220, p. 191–213.

Piccoli, P., Candela, P., Rivers, M., 2000, Interpreting magmatic processes from accessory phases: titanite-a small-scale recorder of large-scale processes: Transactions of the Royal Society of Edingbergh: Earth Sciences, v. 9, p. 257-257.

Plouffe, A., Paulen, R.C. and Smith, I.R., 2006, Indicator mineral content and geochemistry of glacial sediments from northwest Alberta (NTS 84L, M): new opportunities for mineral exploration: Alberta Geological Survey Special Report 77, Geological Survey of Canada, Open File 5121.

Pouchou, J.L., and Pichoir, F. (1985): PAP φ(ρZ) procedure for improved quantitative microanalysis: in Armstrong, J.T. (ed.), Microbeam Analysis, San Francisco Press, San Francisco, pages 104-106.

Rabbia, O.M., Hernández, L.B., French, D.H., King, R.W., and Ayers, J.C., 2009, The El Teniente porphyry Cu–Mo deposit from a hydrothermal rutile perspective: Mineralium Deposita, v. 44, p. 849–866

Roegge, J.S., Logsdon, M.J., Young, H.S., Barr, H.B., Borcsik, M., and Holland, H.D., 1974, Halogens in apatite from the Providencia area, Mexico: Economic Geology, v. 69, p. 229-240.

Rusk, B.G., Reed, M.H., Dilles, J.H., and Kent, A.J.R., 2006, Intensity of quartz cathodoluminescence and trace-element content in quartz from the porphyry copper deposit at Butte, Montana: American Mineralogist, v. 91, p. 1300-1312.

Russell, J.K., Dipple, G.M., Lang, J.R. and Lueck, B., 1999, Major-element discrimination of titanium andradite from magmatic and hydrothermal environments: an example from the Canadian Cordillera; European Journal of Mineralogy, v. 11, p. 919–935.

Schaltegger, U., 2007, Hydrothermal zircon: Elements, v. 3, p. 51–79.

Schand, E.S. and Gorton, M.P., 2004, A textural and geochemical guide to the identification of hydrothermal monazite: criteria for selection of samples for dating epigenetic hydrothermal ore deposits: Economic Geology, v. 99, p. 1027–1035.

Schwartz, G.M., 1953, Geology of the San Manuel copper deposit, Arizona: United States Geological Survey, Professional Paper 256, 65 p.

Scott, K.M., 2005, Rutile geochemistry as a guide to porphyry Cu-Au mineralization, Northparkes, New South Wales, Australia; Geochemistry: Exploration, Environment, Analysis, v. 5, p. 247–253.

Selby, D., Nesbitt, B.E, Muehlenbachs, K., and Prochaska, W., 2000, Hydrothermal alteration and fluid chemistry of the Endako porphyry molybdenum deposit, British Columbia: Economic Geology, v. 95, p 183-202.

Sha, L.K., and Chappell, B.W., 1999. Apatite chemical composition determined by electron microprobe and laser-ablation inductively coupled plasma mass spectrometry, as a probe into granite petrogenesis: Geochimica et Cosmochimica Acta, v. 63, p. 3861– 3881.

Sillitoe, R.H. and Sawkins, F.J., 1971, Geologic, mineralogic, and fluid inclusion studies relating to the origin of copper-bearing tourmaline breccia pipes, Chile: Economic Geology, v. 66, p. 1028-1041

Sillitoe, R.H., 2000, Gold-rich porphyry deposits: Descriptive and genetic models and their role in exploration and discovery: Reviews in Economic Geology, v. 13, p. 315–345.

Sketchley, D.A., Rebagliati, C.M. and DeLong, C., 1995, Geology, alteration and zoning patterns of the Mt. Milligan copper-gold deposits: in Porphyry Deposits of the

Northwestern Cordillera of North America, T.G. Schroeter (ed.), Canadian Institute of Mining and Metallurgy, Special Volume 46, p. 650–665.

Slack, J.F., 1982, Tourmaline in Appalachian-Caledonian massive sulphide deposits and its exploration significance: Transactions of Institute of Mining and Metallurgy, Section B, v. 91, p. B81-B89.

Slack, J.F., 1996, Tourmaline association with hydrothermal ore deposits: in Boron: Mineralogy, Petrology and Geochemistry, E.S. Grew and L.M. Anovitz (ed.), Mineralogical Society of America, Reviews in Mineralogy, v. 33, p. 559–643.

Streck, M.J. and Dilles, J.H., 1998, Sulfur evolution of oxidized arc magmas as recorded in apatite from a porphyry copper batholith: Geology, v. 26, p. 523–526.

Taylor, B.E., and Slack, J.F., 1984, Tourmalines from Appalachian-Caledonian massive sulfide deposits: Textural, chemical, and isotopic relationships: Economic Geology, v. 79, p, 1703-1726.

Tepper, J.H. and Kuehner, S.M., 1999, Complex zoning in apatite from the Idaho batholith: a record of magma mixing and intracrystalline trace element diffusion: American Mineralogist, v. 84, p. 581–595.

Tosdal, R.M., Jackson, M., Pass, H.E., Rees, C., Simpson, K.A., Cooke, D.R., Chamberlain, C.M. and Ferreira, L., 2008, Hydrothermal breccia in the Mount Polley alkalic porphyry copper-gold deposit, British Columbia: in Geoscience BC Summary of Activities 2007, Geoscience BC, Report 2008-1, p. 105–114.

Villeneuve, M., Whalen, J.B., Anderson, R.G. and Struik, L.C., 2001, The Endako batholith: episodic plutonism culminating in formation of the Endako porphyry molybdenite deposit, north-central British Columbia: Economic Geology, v. 96, p. 171–196.

Ward, B., Maynard, D., Geertsema, M. and Rabb, T., 2009, Ice-flow history, drift thickness and drift prospecting for a portion of the QUEST Project area, central British Columbia (NTS 093G, H [west half], J): in Geoscience BC Summary of Activities 2008, Geoscience BC, Report 2009-1, p. 25–32.

Warnaars, F.W., Holmgren, C.D. and Barassi, S.F., 1985, Porphyry copper and tourmaline breccias at Los Broncos-Rio Blanco, Chile: Economic Geology, v. 80, p. 1544-1565.

Watanabe, Y., and Hedenquist, J.W., 2001, Mineralogic and stable isotope zonation at the surface over El Salvador porphyry copper deposit, Chile: Economic Geology, v. 96, p. 1775–1797.

Watson, J.L., 1969, Garnets of the Stikine copper's Galore Creek porphyry: B.Sc. thesis, University of British Columbia, 34 p.

Waychunas, G.A., 2002, Apatite luminescence: in Phosphates–Geochemical, Geobiological, and Materials Importance, M.L. Kohn, J. Rakovan, J.M. Hughes (eds.), Mineralogical Society of America, Reviews in Mineralogy and Geochemistry, v. 48, p. 710–742.

Whalen, J. B., Anderson, R. G., Struik, L. C., and Villeneuve, M. E., 2001. Geochemistry and Nd isotopes of the François Lake plutonic suite, Endako batholith: host and progenitor to the Endako molybdenum camp, central British Columbia; Canadian Journal of Earth Sciences, v. 38, p. 603-618.

Williams, S.A. and Cesbron, F.P., 1977, Rutile and apatite: useful prospecting guides for porphyry copper deposits: Mineralogical Magazine, v. 41, p. 288–292.

APPENDICES

APPENDIX 1: List, location and field description of samples.

APPENDIX 2: Results of the Electron Microbe Analysis.